May 2020

Pyrene Pyrimidine Derivatives: Synthesis, Characterization and Applications

John Kihara Mathaga
Louisiana State University and Agricultural and Mechanical College

PYRENE PYRIMIDINE DERIVATIVES: SYNTHESIS, CHARACTERIZATION AND APPLICATIONS

A Thesis

Submitted to the Graduate Faculty of the
Louisiana State University and
Agricultural and Mechanical College
in partial fulfillment of the
requirements for the degree of
Masters of Science

in

The Department of Chemistry

by
John Kihara Mathaga
B.Sc Kenyatta University, 2004
August, 2020

ACKNOWLEDGEMENT

I am truly appreciative for all those I have encountered in graduate school especially the following: Professor Isiah M. Warner for the excellent mentorship, guidance, encouragement, and financial support you provided for my research. The experience that I have acquired from Warner laboratory will be of great help for my future endeavors. Thesis committee members, Dr. Megan Macnaughtan and Dr. Louis H. Haber for their guidance and support in this journey. Warner group post-docs and group members for there numerous support. My family and friends for their emotional, moral and financial support.

TABLE OF CONTENT

LIST OF TABLES

LIST OF FIGURES

ABSTRACT

In this thesis, development of new materials to the field of optoelectronics were studied. Optoelectronic devices based on organic semiconductors in order to replace their inorganic counterparts have been an increasing focus of research in recent decades. Organic light-emitting diodes (OLEDs) have gained commercial acceptance for their potential use in high-resolution displays and solid-state lighting. This general acceptance is despite the fact that organic electronic concepts (solar cells, transistors and detectors) are still in an early stage of development. OLEDs materials intrinsic advantages, like low power consumption as compared to LED counterparts, a tunable color range, ease of manufacturing, and flexibility have facilitated their exploitation for next generation consumer electronics. However, OLEDs have not fully actualized in the market due to limited life spans, especially in regard to blue color. Thus, in order for these devices to reach their full potential, significant advances need to be made to improve the fundamental limitations cited above.

Based on literature references, blue light has been shown to lag behind red and green lights in terms of stability, and thus, applicability. In this research, compounds from electron deficient pyrimidine derivatives and electron rich pyrene moieties, which can provide deep blue fluorescence, were designed, synthesized and characterized. Characteristics such as thermostability, photostability, UV-absorbance, fluorescence, energy band gaps, Commission Internationale de l'éclairage (CIE) co-ordinates, and quantum yield were studied in this thesis

CHAPTER 1. INTRODUCTION

1.1. Organic Light Emitting Diodes (OLEDs) – A Brief Introduction

Over the past three decades, organic electroluminescence has been one of the most appealing research topics in industry and academia. The captivation of this OLEDs field emanates principally from increase in interdisciplinary research, which include areas such as electrical engineering, device physics, synthetic and physical chemistry, among others.[1] Organic semiconductors are extensively used in optoelectronic applications; most notably, in photovoltaic[2], phototransistors[3], and light emitting diodes (LEDs).[4, 5] Among these, OLEDs comprise a novel and thrilling emissive display technology for next generation full-color, energy saving, flat-panel, electrical displays and illumination. Emissive materials used in OLEDs have several benefits over conventional lighting materials, liquid crystal displays (LCDs), and inorganic light emitting diodes (LEDs). These benefits entail self-emitting properties, wide viewing angles of greater than 170°, wider color ranges, semi-transparency, high resolution and contrast, increased flexibility, rapid response time, low power consumption and overall weight.[6, 7, 8]

In general, an OLED is composed of one or several emitting organic thin coatings inserted between an anode and a cathode.[9] A basic representation for a typical OLED device is exhibited in Figure 1.1. Organic semiconductors, indicated as the organic layer in Figure 1.1, for the fabrication of OLEDs are broadly categorized as polymer light emitters, or higher molecular weight materials, and small molecule emitters, or materials of low molecular weight.

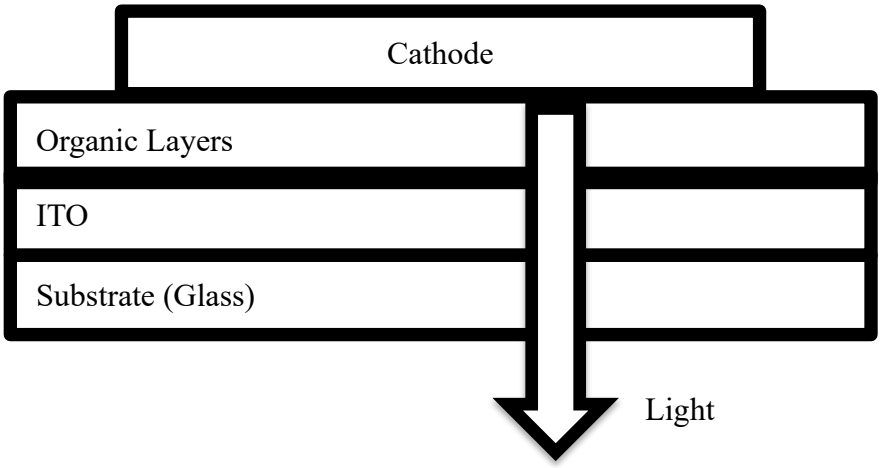

Figure 1.1. Typical OLED structure

1.2. The Organic Emissive Layer

The significant component in OLEDs is the emissive organic layer indicated in Figure 1.1. Owing to their outstanding luminescent properties, as well as their extremely efficient light radiation in the visible electromagnetic spectrum, organic substances have appealed to the attentiveness of most scientists as a light source.[10] This emissive organic film traditionally contains a material with conjugated π-bonds, which could be small molecules or polymers.[10, 11] Typical examples of organic emissive materials are presented in Figure 1.2.[12] These molecules encompass chemical clusters known as "chromophores" that absorb incident light and radiate in the visible region.

The type of emitted light is reliant upon the specific chemical structure of organic layers. Red-green-blue (RGB) radiative materials can be combined to generate a complete color continuum. Therefore, three-color emissive layers have been investigated in the past and continue to be the center of interest in both polymers and small molecules, for actualizing OLEDs display and solid-lighting technology with optimal device efficiency. Blue emissive material, however, present more drawbacks as compared to red and green emitter performance;

for example, external quantum efficiency (EQE) is less than 5% for blue in comparison with red and green emitters that have EQEs greater than 20%.[13, 14]

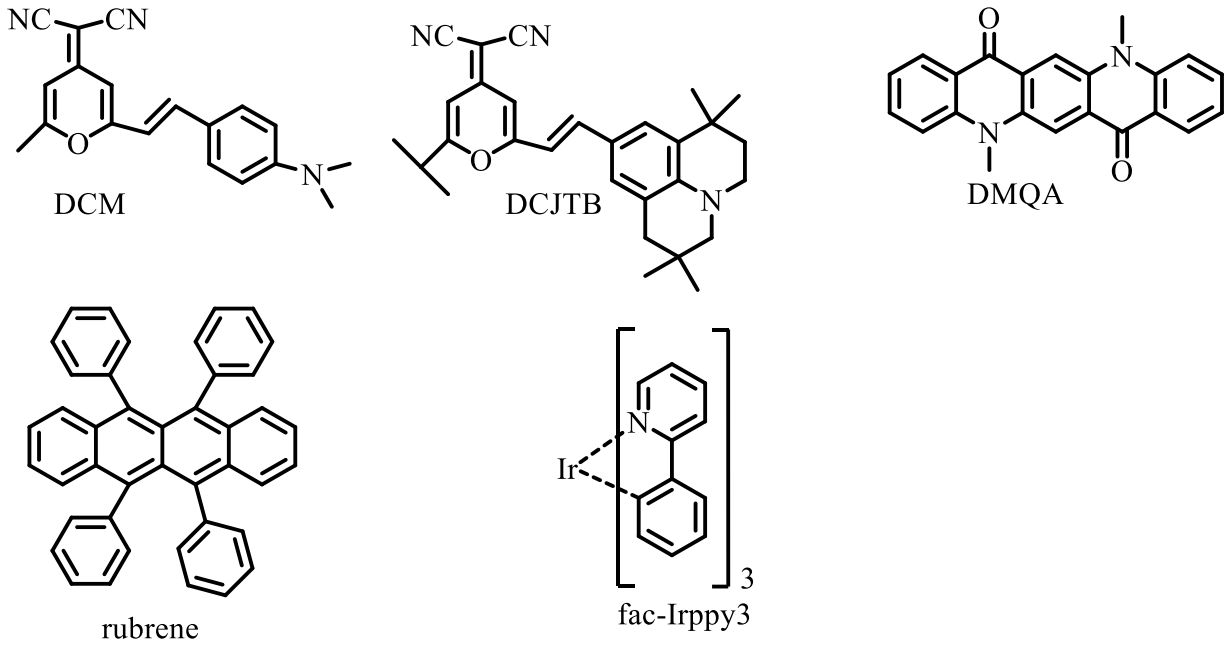

Figure 1.2. Examples of emissive materials; 4-dicyanomethylene-2-methyl-6-p-dimethylaminostyryl)-4 H-pyran (DCM), 4-(Dicyanomethylene)-2-t-butyl-6-(1,1,7,7-tetramethyljulolidyl-9-enyl)-4H-pyran (DCJTB), dimethylquinacridone (DMQA) and fac tris-(2-phenylpyridine) iridium (fac-Irppy3)

Lifespans for blue emitters are typically very low (less than 20,000 hours), which implies that blue emitters degrade rapidly. This rapid deterioration is due to an inherently wide bandgap. Bandgap is defined as the distance between the uppermost occupied molecular orbital (HOMO) and lowest unoccupied molecular orbital (LUMO).[14] A common reason behind rapid degradation of blue emitters has been attributed to the fast bond cleavage of the host materials used in these devices. Host materials used in blue emitters generally have a wide band gap. This remains as a major drawback to commercialization of OLED technology and calls for further research on blue emitters, which is the focus of the study of this thesis.

1.2.1. Polymers for Light Emitting Diodes

Polymers are defined as materials that are composed of lengthy sequences of repeat units of a monomeric compound.[15] Often, when these repeating units are composed of a conjugated carbon chain, the material can show emissive and semiconducting properties.[16] Semiconducting polymers were first discovered by Heerger, MacDiarmid and Shirakawa in 1977.[17, 18] Since then, potential use of these polymers in OLEDs has been investigated by Burroughes *et al.* in 1990.[19] Polymer light emitting diodes (PLEDs) are comprised of an electroluminescent emissive material that gives off light when connected to a source of power. These emissive polymers are normally used as coatings for full-spectrum color exhibitions, which require a relatively small quantity of power to generate light.[20] Even though PLEDs have shown remarkable efficiency in OLEDs application, their synthesis, purification and fabrication as thin films remains a challenge; these drawbacks are primarily overcome using small compounds, as investigated in this thesis, and which could result in attractive competitors.[21]

1.2.2. Small Molecules

Small molecule emitters for OLEDs applications (SM-OLEDs) commonly use materials with low molecular weights.[22] Prof. Ching W. Tang was first to establish remarkable OLEDs using small molecules at Eastman Kodak.[23] In most instances, organometallic coordination complexes and conjugated dendrimers are the type of molecules that are typically used in SM-OLEDs.[24] Differing from PLEDs, SM-OLEDs can be fabricated through vapor deposition, and hence, extremely convoluted multi-layer structures may be constructed.[25] This extraordinary flexibility in stratum design is the principal cause for high efficiencies of the SM-OLEDs.[26] In addition, emissive materials such as pyrenyl-pyrimidine for SM-OLEDs application are generally easier to synthesize and purify than PLEDs. Chapter 2 of this thesis focuses on the

synthesis and characterization of small molecules with blue emission for potential OLEDs applications.

1.3. Fluorescent Blue-Emitters

The research work presented in Chapter 2 of this thesis focuses on development of candidates for blue-emitting materials in OLEDs. Ideally, red-green-blue (RGB) should yield equivalent pigment purity, operative lifespan, and efficiency for OLED technology to be actualized.[27] However, the wide band gap of blue emitters affect well-organized charge injection.[28] This leads to a rapid degradation of emissive layer upon excitation.[28] As a result, blue-emitters tend to have the following limitations: lower operational lifetime, lower efficiency, and lower spectral purities, creating a large obstacle to fully commercialize OLED technology.[29]

Blue fluorescent emitting layers exist in two forms (i) doped and (ii) non-doped. Doped systems are usually designed by integrating blue incandescent pigments in emissive materials to prevent fluorescence quenching. This blending strategy often suffers from limitations due to aggregation of dopants and phase separation as a result of incompatibilities of materials. Non-doped systems, which are discussed in more detail in Chapter 2, are a strategy that has demonstrated elimination of complications like phase separation and concentration-based quenching. However, challenges such as low charge injection and passage emanating from the inherent large energy gap persist still.[30, 31]

1.3.1. Non-doped Blue Emitters

In order to investigate diverse types of blue fluorescence emitters for non-doped SM-OLEDs materials based on di(styryl)arylene, carbazole, anthracene, phenanthrene, tryphenylamine, fluorene, and pyrene have been synthesized to improve on their electroluminescence (EL) characteristics (Figure 1.3).[32-36] Anthracene derivatives have been

developed and investigated in the literature as a blue emissive material owing to their good photoluminescence (PL) properties in solution, as well as emission with reduced luminescent quenching in solid films.[37] Incorporating different moieties that are mostly electron deficient that can facilitate the electron transportation within the system, modifies these blue fluorophores by promoting electron localization within the system.[38] For instance, Shu *et al.*, have shown a remarkable photoluminescence quantum yield (PLQY) of approximately 0.89 relative to DPA, a precursor, in solid state for 2-tert-butyl-9,10-bis[4-(1,2,2-triphenylvinyl)phenyl]anthracene (TPVAn) (Figure 1.4).[39] This value is a dramatic increase from the PLQY value obtained from diluted solution (0.06). This high PLQY value from TPVAn was ascribed to restricted intramolecular motion of phenyl rings in the solid state, which may translate to a higher EQE of the emitter material.[40]

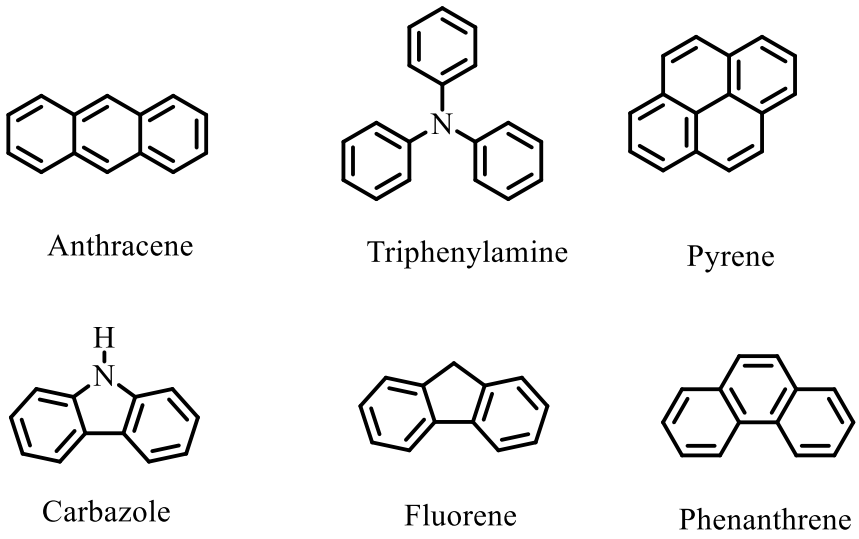

Figure 1.3. Blue fluorescent emitters using nondoped SM-OLEDs

Furthermore, due to their high PLQYs and enhanced thermal- and photo-stabilities, anthracene- and fluorene- containing molecules have also been extensively investigated as possible blue emissive materials.[41] Nonetheless, fluorene-based devices have red-shifted (long-wavelength) emissions that emanate mostly from electro-oxidized cleavage or photo cleavage of

C9-substituted alkyl pendent cluster(s).[42] This red shifted emission leads to degraded pigment purity. To address this issue, Wong *et al.*, designed ter(9,9-diarylfluorene) (TDAF), in which the aryl group afforded hindrance on the interchromophore. This molecule exhibited high PLQY of 0.9 in the solid state.[43, 44]

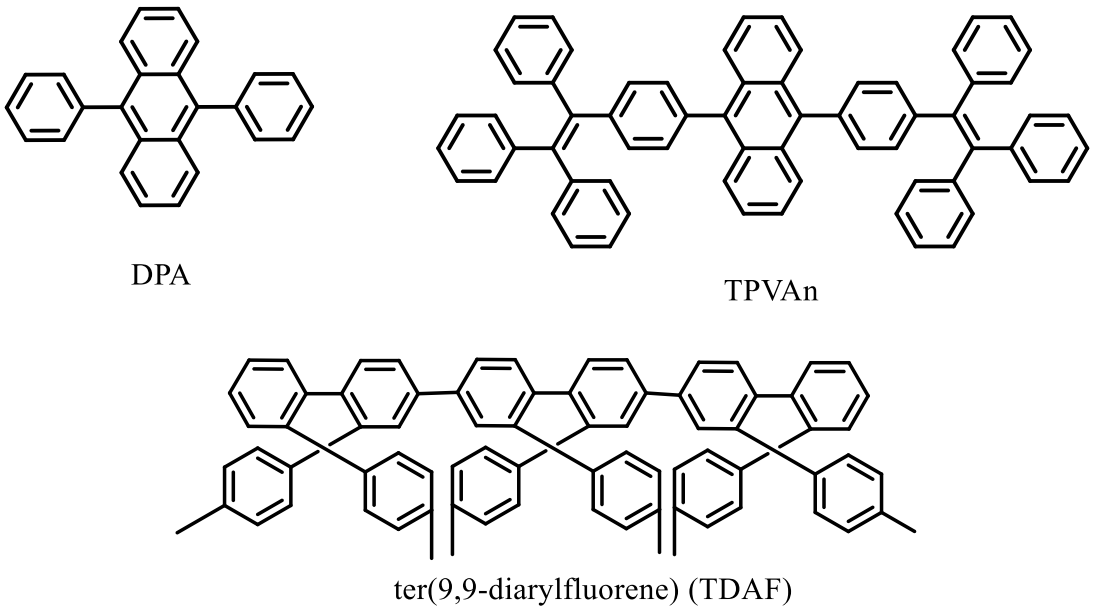

Figure 1.4. 9,10-diphenylanthracene (DPA), TPVAn and TDAF

Carbazole, shown in Figure 1.3, is another blue emitter that has gained attention as a significant component of organic material for OLEDs application due to its propensity for blue emission.[45] Therefore, numerous researchers have focused on properties centered on the carbazole unit. For instance, phenothiazine and pyrenyl-carbazole-based electroluminescent OLEDs were developed by Salunke *et al.*[46] Carbazole-derived ***g***roup of ***u***niform ***m***aterials ***b***ased on ***o***rganic ***s***alts (GUMBOs) has also been developed by Siraj *et al.*, and have shown remarkable properties for blue emission, such as enhanced PLQY and EQEs values.[47]

1.4. Multifunctional Non-doped Blue-Emitters

As mentioned earlier, the electroluminescence properties of blue emitters usually suffer from stunted charge injection and conveyance in the emissive layer. In order to obtain high

efficiencies in blue OLEDs, optimization of charge balance has to be achieved.[41] Normally an emissive layer featured with enhanced charge injection and conveyance properties can effectively elevate device performances.[48] Thus, appropriate blue emitters should possess excellent charge carrier conveyance capabilities to provide a balanced stream of electrons and holes to emissive material in a simplified device structure.[41, 48] Due to these necessary characteristics, electron and/or hole conveyance units may be built into the blue-emitting molecule.

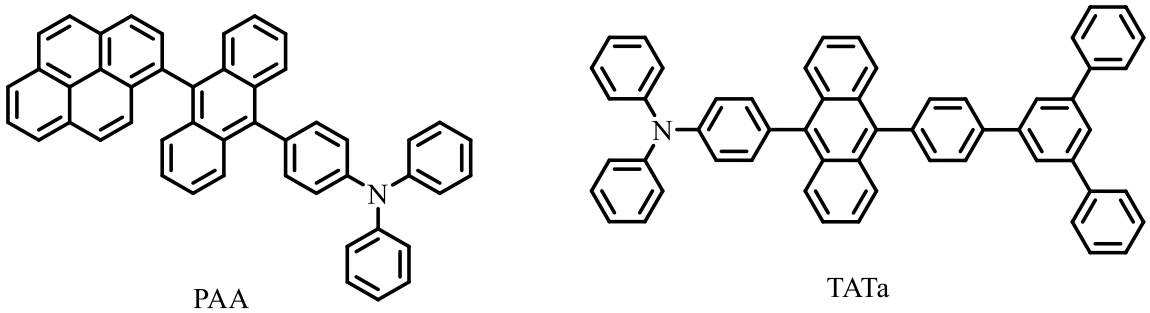

PAA TATa

Figure 1.5. Examples of P-type non-doped blue fluorescent materials: 9-pyrenyl-10(4-triphenylamine)anthrancene (PAA) and 4-(10-(3',5'-diphenylbiphenyl-4-yl)anthracen-9-yl)-N,N-diphenylaniline (TATa)

1.4.1. P-type vs. N-type Non-doped Blue-Emitters

P-type compounds are molecules that are covalently attached to blue fluorophores during synthesis and add or enhance good hole-transporting abilities through an electron-rich species. Triarylamine groups, for instance, enhance hole transport via highly stable radical cation species.[49] These groups have also been increasingly incorporated into molecules and provide bulky compounds with higher thermal stability.[49, 50] In this thesis, focus is on the N-type non-doped blue fluorescent emitters, which incorporate electron-accepting molecules into the matrix and are discussed in more detail below.

Electron-accepting material, such as indenopyrazine[51], quinoline[52], imidazole[53,54,55] pyridine[56] and pyrimidine[57] (Figure 1.6), have been exploited in the past to develop novel N-type

RGB emitters. All of these electron-accepting moieties, when covalently linked to the emissive materials, such as carbazole, anthracene, pyrene etc., have shown remarkable properties for OLEDs application.[58] For instance, Park *et al.,* have shown that by incorporating indenopyrazine to emissive layer facilitates electron injection and transportation leading to a deep blue emitting material.[59]

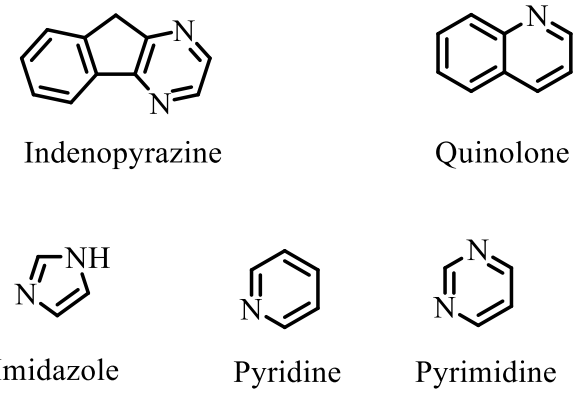

Figure 1.6. Electron accepting materials

1.4.2. Pyrene as a Blue Emitter

Pyrene is a relatively small polycyclic hydrocarbon comprised of four aromatic rings. The name "pyrene" originates from the antique Greek word "π υ ρ" which denotes fire, as the French organic chemist Auguste Laurent was convinced that pyrene was produced whenever organic matter was burned. Pyrene presents an intense native deep blue fluorescence in cyclohexane solution with a maximum emission wavelength at 380 nm and a PLQY in EtOH of 0.65.[60] For this reason, pyrene was chosen as the blue fluorophore in this thesis. Moreover, pyrene has been shown to possess high photo- and thermal-stability, which are appealing characteristics for emissive layers.[61] Despite pyrene exhibiting these desired qualities for blue OLEDs application, it is known to present poor charge transport mobility and has a robust propensity for forming crystalline excimers.[62,63] It has been shown in the literature that pyrene-pyrene excimers have a significant bathochromic shift in fluorescence emission of roughly 30 to

40 nm, which leads to a shift from “deep-blue” to “sky-blue;” hence, degrading the color purity.[64]

In order to disrupt excimer formation of pyrene molecules, derivatives should be carefully designed. An unadorned and effective approach to suppressing excimer formation has been demonstrated by use of tetra(o-tolyl)pyrene (TOTP).[65] Poly-pyrenes prepared by 1-3-polymerization[66] or pyrene core based poly-phenylene dendrimers[67,68] have also been designed to prevent pyrene-pyrene stacking, thus providing excellent suppression of excimer formation with the shortcoming that OLEDs are most often processed in solution. In addition, these polymers demand significant synthetic prowess and complex purification processes. A simple, but efficient, *tert*-butylcarbazole substituted pyrene derivative has been demonstrated by Kaafarani *et al.,* for solution fabricated OLEDs.[69] Recently, De Silva *et al.* have developed deep blue emitters by integrating pyrene moieties with a pyridine core, that presents superb optical properties, enhanced thermal stability, and increased PQLY and EQE.[70] Novel pyrenyl-pyrimidine compounds were synthesized and compared to previously reported materials in this thesis. The conjugated incorporation of electron-accepting pyrimidine is anticipated to assist in reduction of pyrene aggregation and improve color stability in the solid state. Preliminary results have indicated the possibility of using pyrenyl-pyrimidine conjugates in the fabrication of OLEDs as robust blue emissive layers.

1.5. Analytical Techniques Used in This Research

1.5.1. Ultraviolet-Visible Spectroscopy (UV-vis)

Ultraviolet-Visible Spectroscopy (UV-vis) is a characterization procedure for analyses of molecules that absorb light in the ultraviolet and visible region of the electromagnetic spectrum. In this technique, a beam of light is passed through an analyte sample causing a reduction in the

intensity of light due to absorption of it by the analyte.[71] Upon analyte absorption, common electronic transitions of organic compounds may occur, such as pi-bonding to pi-antibonding (π-π*), non-bonding to pi-antibonding (n-π*), non-bonding to sigma anti-bonding (n-σ*), π-σ*, and σ-σ*, shown in Figure 1.7.[72]

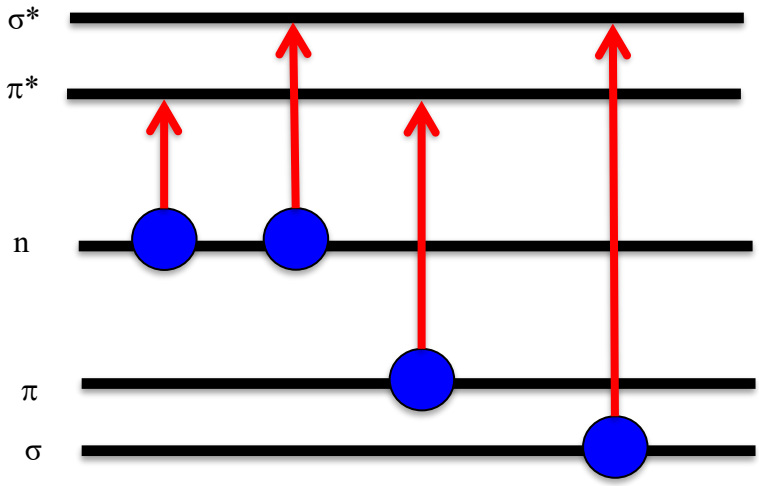

Figure 1.7. Various transitions that emanates from UV-vis absorption spectroscopy

A double beam UV-vis spectrophotometer (Figure 1.8) is often used to measure and record the amount of energy that molecules absorb whenever they are exposed to UV-vis light. The light source (lamp) generates energy, which is passed through a monochromator that select the desired wavelength range. A beam splitter indicated in the diagram divides the light into two beams.

$$A = \epsilon bc \qquad 1.1$$

One of the beams passes through the reference holder and the other through the sample holder simultaneously. A photomultiplier or diode array detector is then used to record the light absorbed or transmitted by the sample. A spectrum is then obtained as a result of plotting the absorbance or transmittance against the wavelength range. The amount of light absorbed, termed

as the absorbance (A) is related to the molar absorptivity (ε), concentration (c) of the analyte as well as the path length of the cuvette (b) by the equation 1.1.[73, 74]

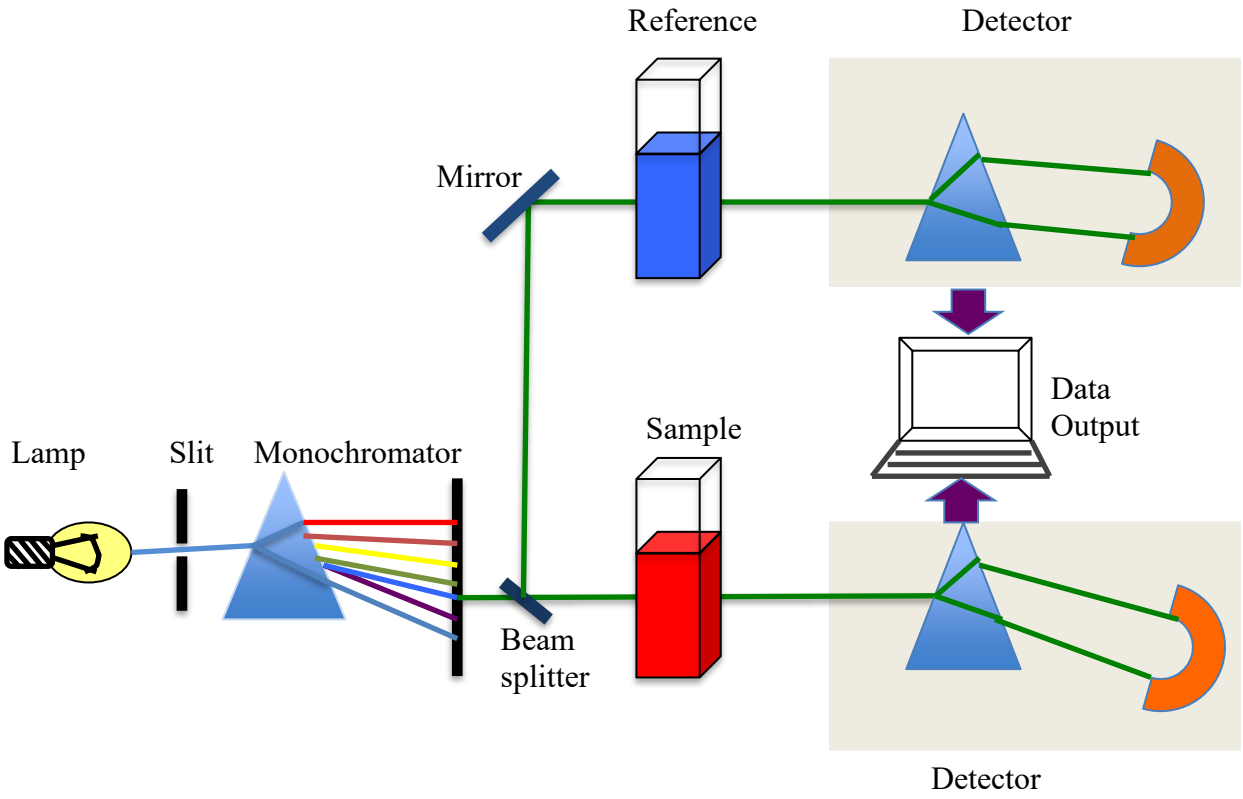

Figure 1.8. Schematic representation of a double beam UV-vis spectrophotometer

15.2. Fluorescence Spectroscopy

Luminescence is defined as the radiative transitions between states of the same multiplicities commonly studied through fluorescence spectroscopy.[75] Luminescence is further subdivided into photoluminescence, electroluminescence, chemiluminescence, radioluminescence, and thermoluminescence based on the excitation source.[76] In this thesis, photoluminescence is elaborated and discussed further as an evaluation for a given fluorophores and is crucial to determining the potential emissive layer of an OLED. Photoluminescence is generally measured using an instrument known as spectrofluorometer, which is schematically presented by Figure 1.9.[77, 78]

A typical spectrofluorometer consists of a light source, excitation and emission monochromators, a sample holder or chamber, and detector that may be a photomultiplier tube or a Charged Coupled Device (CCD). It is worth noting that the 90° configuration in the instrument minimizes incident light reaching the detector. The excitation monochromator allows light of the selected excitation wavelength, to irradiate the sample, which may be in solid state in thin films on quartz glass or solution state inside optically transparent glass cuvettes.

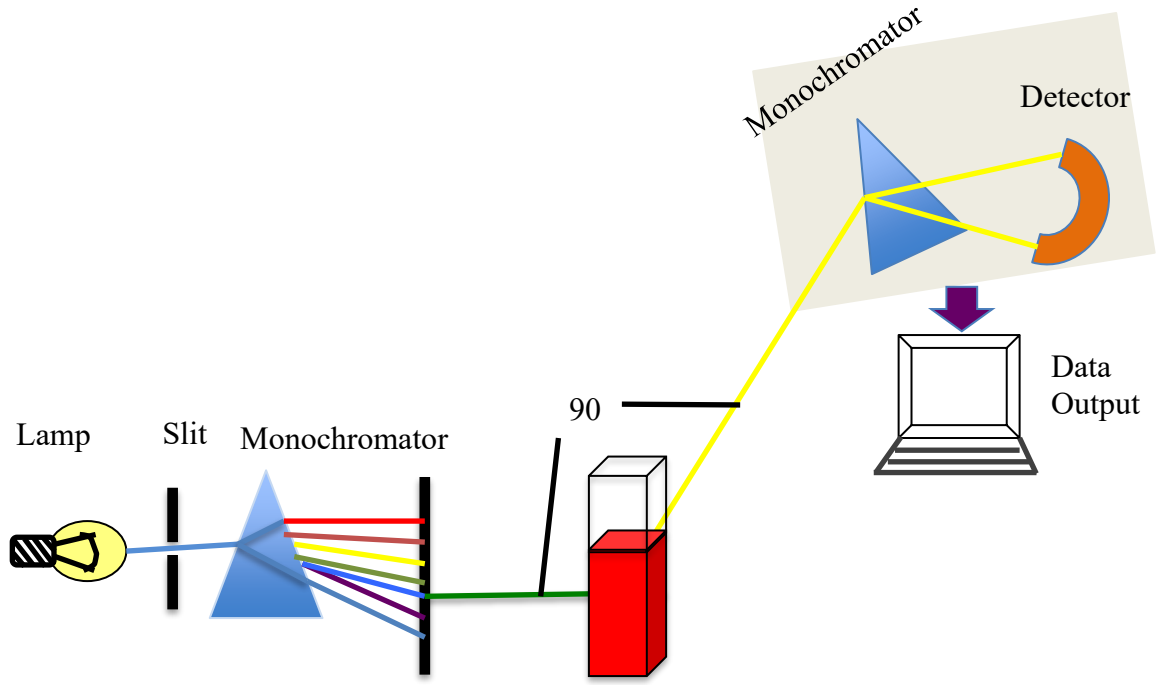

Figure 1.9. Schematic representation of a spectrofluorometer

Commonly used light sources for the spectrofluorometer are lasers, photodiodes, and lamps. The output from the spectrofluorometer is a spectrum of fluorescence intensity versus the wavelength range.[78] Another interesting feature of the emitter materials realized from spectrofluorometer measurements is the "Commission internationale de l'éclairage" “C.I.E” coordinates of the emitter compound.[78-80] Furthermore, spectrofluorometer assists in the determination of PLQY. For the purpose of this thesis, absolute PLQY measurements were done using an integrated sphere that was incorporated to the spectrofluorometer.

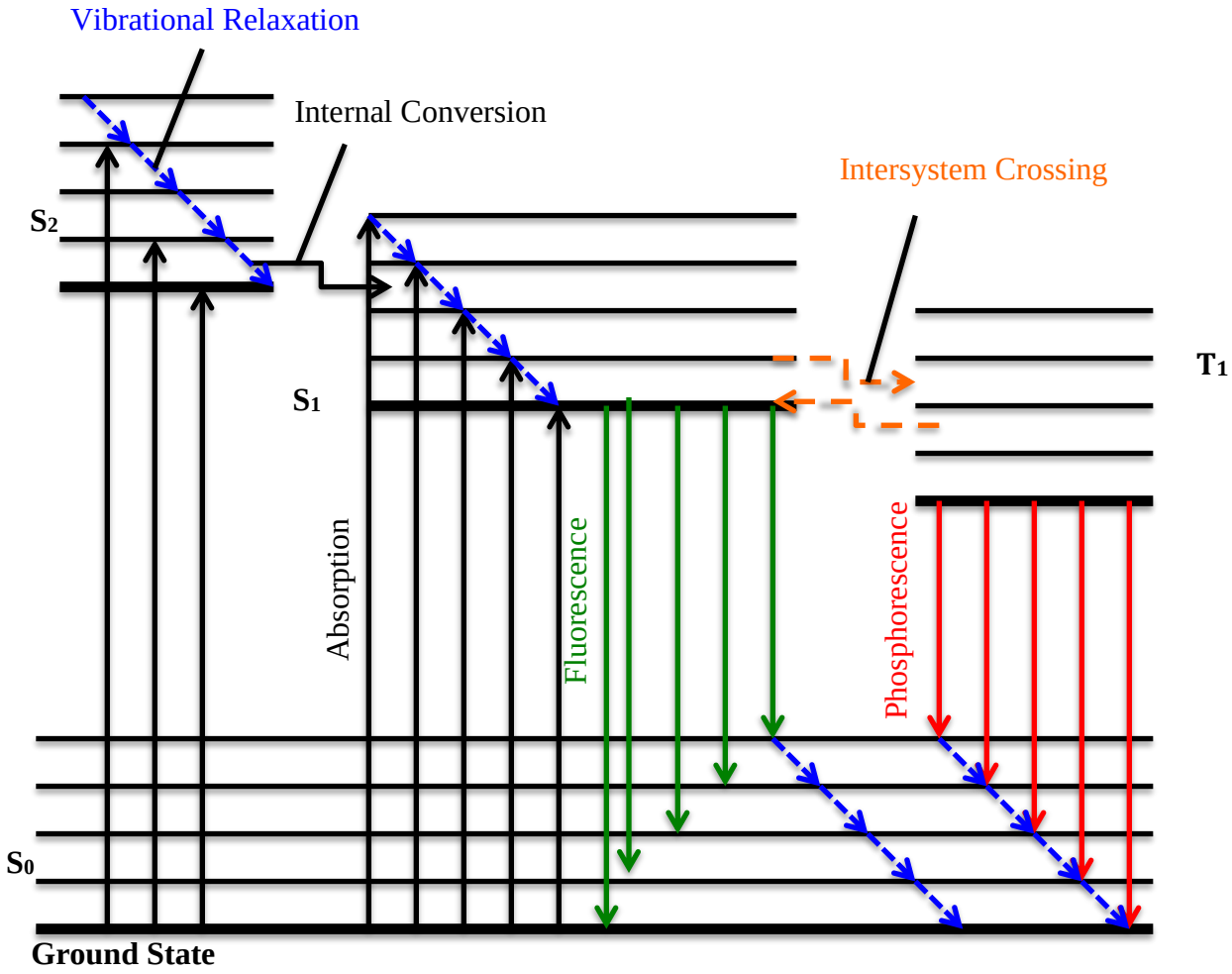

Figure 1.10. Jablonski diagram showing radiative (solid lines) and non-radiative (dashed lines) processes

It is worth noting that fluorescence can occur alongside several other competing processes, which tend to decrease the PLQY and EQE of the emissive material as indicated by a simplified Jablonski diagram shown in Figure 1.10. Molecules can undergo internal conversion, which is a non-radiative transition between a higher to lower energy electronic state (10^{-9} s). Intersystem crossing is another non-radiative process that occurs when there is transition between electronic states of different multiplicity, such as S_1 to T_1 transition with a time flame of 10^{-9} s. This transition is possible whenever the energy of the two states is close enough.

Phosphorescence is another competing process that is a radiative transition that occurs from T_1 to S_0 in most organic molecules with a time flame of $10^{-3} – 10^{-9}$ and harness 75% of exciton as compared to 25% exciton harvested by the fluorescence as shown in table 1.1. Finally, a more recent process that is harnessing 100% exciton is worth mentioning, i.e. thermally activated delayed fluorescence (TADF). This process involves system crossing to and from the triplet before undergoing radiative transition from S_1 to S_0 via fluorescence. This in turn facilitates fluorophores to harvest all excitons from the singlet state and triplet states; thus, yielding 100% harness of excitons.[80-82]

Table 1.1. Approximate duration for intramolecular energy transmission processes

Process	Time, sec
Excitation	10^{-15}
Absorption	10^{-15}
Vibrational relaxation	10^{-12}
Internal conversion	10^{-12}
Fluorescence	10^{-9}
Phosphorescence	$10^{-3} – 10^{-6}$

1.5.3. X-Ray Diffraction (XRD) Studies.

Solid-state and thin-film morphology is very important information for understanding the photophysical properties of EMLs. In different forms of this method, X-rays interacts with the sample in the form of a single crystal, a powder, or a thin film, and diffracts with constructive and destructive interferences determined by Bragg's equation 1.3.[83-85]

$$n\lambda = 2d\sin\theta \quad , \qquad 1.3$$

where n is a constant that is always positive, d is lattice spacing λ is the wavelength of the incident wave, and θ is the scattering angle.

Single powder x-ray diffraction (PXRD), which is a rapid analytical procedure principally used for phase identification of a crystal-like material and can provide information on

unit cells, was employed in this thesis. The material that was probed was finely powdered, homogenized and an average bulky composition determined. All diffraction methods are based on generation of X-ray tube. These X-rays are directed at the samples and the diffracted rays are collected. The fundamental component of all diffraction is normally the angle between the incident and diffracted rays.[85, 86]

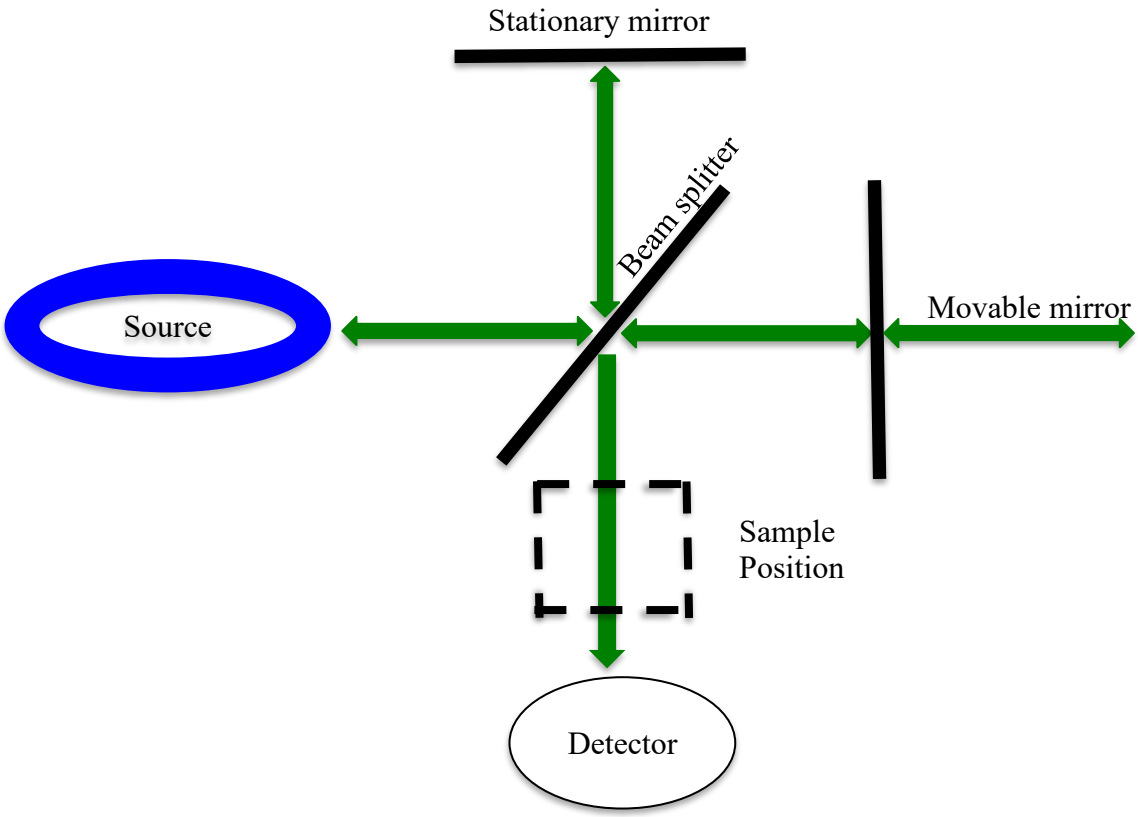

Figure 1.11. Schematic diagram of a typical FTIR

1.5.4. Fourier Transform Infrared Spectroscopy

Fourier Transform Infrared Spectroscopy **(**FTIR) is an analytical technique that is used to give precise and accurate identification to organic compounds, polymeric, and inorganic materials.[87, 88] Infrared light is scanned through the solid or liquid sample in this technique where the spectrum reveals the nature of the chemical investigated.[87] Normally, FTIR instrument, a simplified diagram is presented by Figure 1.1, pass infrared radiation of about 4,000 to 400 cm^{-1}

through a sample, where some of radiation are absorbed and some pass through without being absorbed and a spectrum is generated.[89] The resulting signal at the detector is presented as a spectrum, typically from 4000 cm^{-1} to 400 cm^{-1}, representing a molecular fingerprint of the sample. Each molecule or chemical structure normally produces a unique spectra fingerprint, making FTIR analysis a great tool for structural elucidation.[90-92] Therefore, FTIR was used in this thesis in identifying the chemical structures of the newly synthesized compounds.

1.5.5. Thermogravimetric Analysis (TGA)

TGA is an analytical technique in which the mass of a substance is monitored as a function of temperature or time as the sample specimen is subjected to a controlled temperature program in a controlled program.[93] This technique employs a sample pan that is supported by a precise balance, which resides in a furnace where it is heated or cooled during the experiment.[93, 94] It also consists of an inert or reactive sample purge gas that flows over the sample and exits via an exhaust to control the sample environment. The change in mass of the sample is thus monitored during the experiment; hence this technique can be used to quantify loss of water, loss of solvent, loss of plasticizer, decarboxylation, pyrolysis, oxidation, decomposition etc. A TGA thermal curve is displayed from left to right where the descending TGA thermal curve indicates a weight loss occurred.[93]

1.6. Chromaticity and Color Gamut

The "Commission internationale de l'éclairage" (CIE) color model is a color space model that was created by the International Commission on Illumination known as the Commission Internationale de I'Elcairage (CIE).[95] It is actually a mapping system that uses tri-stimulus values, a combination of the three mathematical functions that represent the primary color values

red, green and blue to generate the observed color, which are plotted in a 3D space. In this way, this model eliminates the chromatic response of the eye; a response that changes as the cones across the retina differ in their response to light and color in different areas of the retina.[96] The CIE color space is dated back to 1931, and is the most accurate color model whose aim is to map out all the colors.[97]

1.7. Scope of Thesis

This thesis is focused on the design, synthesis, and characterization of pyrenyl-pyrimidine derivatives, which present a high potential as blue emissive materials for possible OLEDs applications. Accordingly, chapter two includes two novel blue light emitting compounds, 2,5-dipyrenylpyrimidine and 2,4,6-tripyrenylpyrimidine which were thoroughly evaluated for solution and solid state optical characteristics as well as other properties such as thermal- and photo- stabilities.

CHAPTER 2. DESIGN, SYNTHESIS, CHARACTERIZATION AND SOLID STATE OPTICAL PROPERTIES OF HIGHLY EFFICIENT NOVEL DEEP-BLUE PYRENYL PYRIMIDINE COMPOUNDS

2.1. Introduction

Highly photoluminescent compounds have numerous applications like in sensors,[98] as biomarkers,[99] in organic photo-voltaic (OPV),[100, 101] solar cells, [102, 103] and organic light emitting diodes (OLEDs).[104-106] Recently, emphasis has focused on development and diversification of OPVs and OLEDs technologies with the aim of mitigating the world's energy-shortage problems.[107-110] These technologies have the strategic advantage of harnessing solar energy and low cost manufacturing, respectively. Extensive research has been carried out to promote OLEDs into commercial applications as flat-panel display especially with smart-phone technology explosion, television screens, laptops, monitors, solid-state lighting resources, and more.[111-113] This widespread technology takes advantage of the opportunity provided by π-conjugated systems of polycyclic aromatic hydrocarbons to obtain a desired light source.[114] These π-conjugated systems have energy structures suited for emission in the visible region of the electromagnetic spectrum (EMS).[115] In addition, the ease of tailoring chemical and electronic properties of these structures is relatively simple.[116, 117]

For a full color display and solid lighting, red, green and blue light emitters, of relatively equal stability, efficiency and color purity are required, and these emitters could be either polymers or small organic molecules.[118-120] Small organic molecules for OLEDs are preferred over polymers due to their easier synthesis, purification, characterization, and modification. Red and green emitters have been widely explored, whereas development of blue emitters has lagged in terms of color purity and efficiency.[121] Low-wavelength emitters (i.e. blue emitters) are of particular interest as they are necessary to obtain white light.[122] This lagging in development is a

result of large HOMO-LUMO energy gaps and low electron affinities (EAs), leading to inefficient electron injection into the blue emitters.[123] To compensate for poor electron injection, an additional electron-transport/hole-blocking layer, as well as a low-work-function cathode, can be used.[124] However, this approach suffers from complicated fabrication processes or poor environmental stability of the active materials.[124]

These poor electron injection and transport properties relates to blue emitters that have lower performance properties than red and green emitting layers, since the low electron injection leads to lower external quantum efficiency (EQE) and vice versa. To date, most blue-emitting compounds have an EQE of less than 5% and a lifetime less than 20,000 hours.[125] Comparatively, red and green emitters exhibit 19-20% EQE, and lifetimes reaching approximately100,000 h.[125] Therefore development of high efficiency blue emitters for OLEDs fabrication with longer performance lifetimes is an urgent concern to actualize commercial applications in display and solid state lighting. Along with device performance requirements, blue emitters for OLEDs application require a standard Commission Internationale de L'Eclairage (CIE) coordinate value less than 0.15 along with an (x+y) value less than 0.30.[41] Therefore, it is of great interest in the scientific community to design blue emitting materials with high EAs that also facilitate electron injection and transport.[126]

Compounds that have been used for blue emitting OLEDs fabrication include polycyclic aromatic hydrocarbons (PAHs) based luminophores such as carbazole,[127, 128] anthracene,[129] di(styryl)arylene,[130] perylene,[131] fluorene,[127, 132] and pyrene.[133, 134] Among these luminophores, pyrene provides a great potential for the fabrication of new OLEDs materials owing to its excellent emission properties, strong absorption cross section, which is a measure for the probability of an absorption process, long excited state lifetime, high thermal- and photo-

stabilities, and favorable charge carrier properties.[135] [136] Correspondingly, a number of pyrene derivatives have already been reported as blue- or green- emitters, such as pyrene-functionalized carbazole,[137] pyrene-functionalized triphenylamine,[138] and pyrene-functionalized pyridine.[139] However, the realization of a blue emitter with a lifetime and EQE closer to red and green has not yet been attained.

In this chapter, a blue-emitting target involving the functionalization of pyrene, which has a native deep blue fluorescence, has been proposed. Pyrene by itself as a candidate for a solid-state blue emitter, present certain limitations due to poor charge carrier mobility characteristics and a strong tendency to undergo excimer formation due to π-π* stacking in the solid state.[140, 141] Excimer formation conduces to a significant bathochromic shift in fluorescence emission of approximately 30–40 nm (a shift from "deep-blue" to "sky-blue").[141] Often, pyrene in the condensed state also shows aggregation induced quenching, that diminishes color purity (alters the desired CIE coordinates) and efficiency of the device.[139] Alternatively, in rare cases, some derivatives exhibit aggregation-induced emission (AIE), which takes advantage of the restriction of intermolecular rotation within the structure. This restriction normally enhances the emission efficiency in the condensed solid state.[142] [41]

It is relevant to design blue emitting materials with high EA values and small energy gaps in order to enhance electron injection into the blue emitter.[41] To achieve this, researchers have developed N-type non-doped blue fluorescence emitter materials, which have high EA values hence facilitating electron injection and transport.[41] In addition to facilitating electron injection and transport, compounds through which pyrene are attached may contain moieties that also assist in reducing the aggregation π-π* stacking. To achieve this, pyrene units are mutually twisted into nearly orthogonal conformation with respect to each other. These twisted

conformations electronically isolate individual pyrene moieties within each molecule to minimize π-π* stacking as a result of the increased steric hindrance that prevent face-to-face pyrene aggregation.[143]

To improve upon electronic properties, such as decreasing energy gaps for enhanced electron injection, as well as incorporate torsional strain and intramolecular twisting, electron-accepting moieties have been used as a central ring.[144] Electron deficient molecules such as pyrazine, quinolone, imidazole, phosphine oxide, pyridine, and pyrimidine are covalently linked directly to blue-emitting fluorophores.[145] A series of pyrenyl-pyridines compounds for blue emission have been synthesized and characterized recently by De Silva *et al.*,[146] pyrene-imidazole derivatives have been previously reported for OLEDs,[147] and pyrene-oxadiazoles for OLEDs has also been investigated.[148] [149]

Herein, two novel derivatives of pyrenyl-pyrimidine compounds, namely 2,5-pyrenylpyrimidine (2,5-DPP) and 2,4,6-tripyrenylpyrimidine (TPP), were synthesized. Their properties as potential blue-emitters were studied and compared to 2,4-DPP and 4,6-DPP both in solution and solid state. Novel compounds reported in this study exhibit high thermal stability, desirable emission properties in the solid state, and one isomer were found to have a quantum yield of over 100% in solution. Optical spectra confirm the low HOMO-LUMO energy gap, which also confirms their suitability for their potential use as a hole-transport layer in light emitting devices. The low energy band gap ranges between 1 to 1.5 eV while the high band gap ranges between 2 to 4 eV.[150] From the results obtained from this study, the new compounds portrayed good traits for possible application as blue emitters for OLEDs devices.

2.2. Experimental Methods

2.2.1. Materials and Reagents

Pyrene-1-boronic acid, 2,4,6-trichloropyrene, 2,4-dichloropyrimidine, 2,5-dichloropyrimidine and 4,6-dichloropyrimidine were purchased from Tokyo Chemical Industries Co. Ltd. (Portland, OR) and 1,4-dioxane was purchased from Acros Organics (West Chester, PA). Tetrakis (triphenylphosphine) palladium(0), bis(triphenylphosphine) palladium (II) dichloride ($Pd(PPh_3)_2Cl_2$ were all bought from Sigma-Aldrich (St. Louis, MO). Potassium carbonate (K_2CO_3) was procured from Fisher Scientific (Fair Lawn, NJ). Chloroform ($CHCl_3$), tetrahydrofuran (THF), acetone, isopropanol, ethanol, ethyl acetate (EA), hexane, ethyl acetate (EtOAc), dimethyl sulfoxide (DMSO), acetonitrile (ACN), toluene, dichloromethane (DCM) and methanol (MeOH) were purchased from Macron (Center Valley, PA). All chemicals were used as received without further purification. Column chromatography was performed on silica gel (Sorbent Technologies, 60 Å, 60-63 μm) slurry packed in glass columns. Quartz glass was acquired from SPI supplies and used to prepare solid films.

2.2.2. Instrumentation.

Absorbance measurements were performed using a scanning spectrophotometer (UV-3101PC, Shimadzu, Columbia, MD), and fluorescence emission was measured on HORIBA Spex Fluorolog-3-spectrofluorometer (model FL3-22TAU3; Jobin-Yvon, Edison, NJ). In order to measure photostability, a 450Watt lamp of the fluorometer (FL-1039/40) was used as light source with entrance and exit slit widths maintained at 14 nm. The photostabilities of each compound, both in solution and solid state (thin film) were studied over a period of 3600s by exciting at their respective absorption maxima and measuring their fluorescence at their emission maxima. An integrating sphere (150 mm internal diameter) was used to measure the absolute

quantum yields for solution and film samples by connecting the fluorometer to Horiba Scientific Quanta φ accessory (model FL3-22TAU3; HORIBA Scientific, Edison, NJ), with entrance and exit slit widths maintained at 3-5 nm and using quartz cuvettes (Starna Cells) with path lengths of 1cm. For the photoluminescence quantum yield (PLQY) measurements, the slit width was opened to 3-5 nm and filters (CVI optic filters, HORIBA Scientific) on both the entrance and exit were used, this was achieved by connecting an integrating sphere to the fluorimeter. Thermal stability studies were performed with a Hi-Res Modulated TGA 2950 Thermogravimetric Analyzer (TA Instruments, New Castle, DE). Samples were heated gradually from room temperature to 600 °C at a rate of 10 °C per minute. The values of the inception temperature were determined using TA Universal Analysis software and reported as the decomposition temperatures (T_d) from 5% weight loss. MPA160 melting point apparatus (Stanford Research Systems, Inc., Sunnyvale, CA) was employed to determine the melting point of synthesized compounds Powder X-ray diffraction analysis was performed with a Panalytical Empyrean multipurpose diffractometer (Westborough, MA). Solid films were prepared using a spin coater model WS-650 MZ-23NPPB with static mode at a spin rate of 600 rpm and duration of 30s.

2.3. Synthesis and Characterization

2.3.1. General Syntheses of Pyrenyl-Pyrimidine Derivatives

A one-step Suzuki coupling reaction between chloro-pyrimidine and pyrene-1-boronic acid was used to synthesize four pyrenyl-pyrimidine compounds namely 2,4-DPP, 4,6-DPP, 2,5-DPP, and TPP. A previously reported synthesis of 2,4-DPP and 4,6-DPP was followed with slight modification and was adapted for 2,5-DPP and TPP.[151] A schematic of the synthetic path of TPP and structures of four synthetized compounds are shown in Figure 2.1. Further details of their synthesis and purification can be found in the Appendix section.

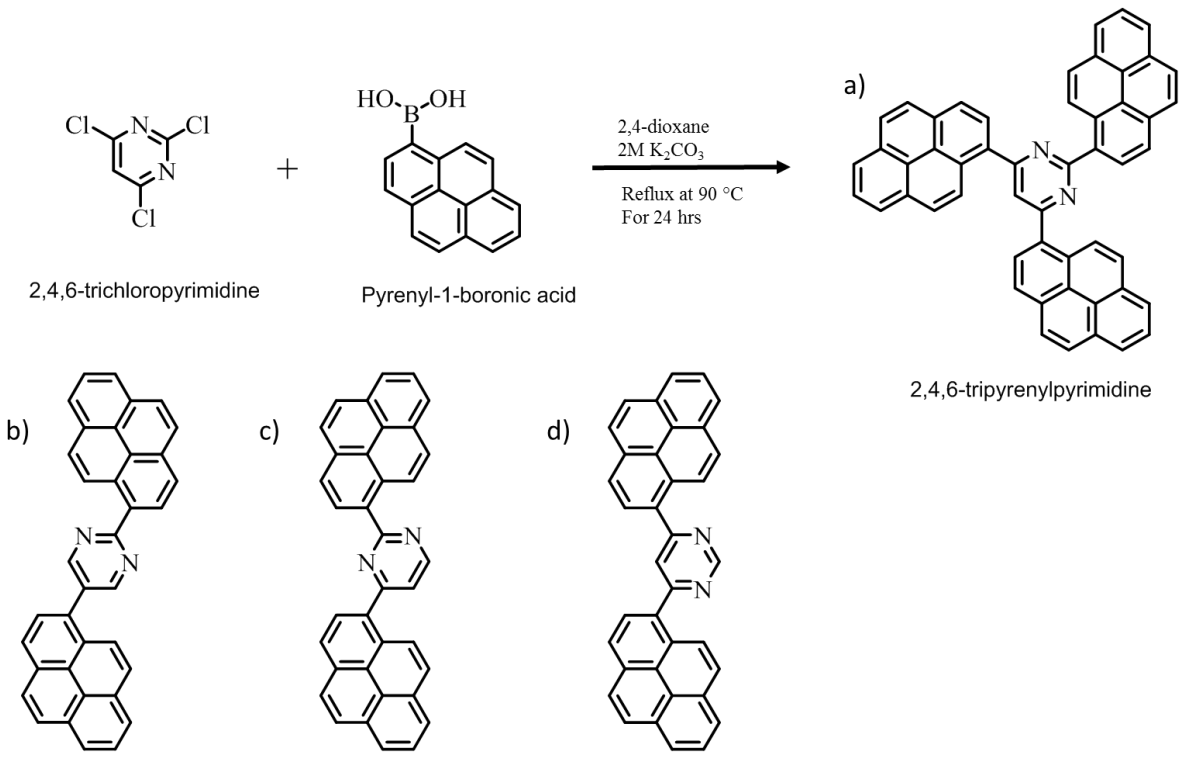

Figure 2.1. Synthesized Compounds (a) 2,4,6-tripyrenylpyrimidine (TPP), and the dipyrenyl pyrimidine synthesized, (b) 2,5-dipyrenylpyrimidine (2,5-DPP), 4,6-dipyrenylpyrimidine (4,6-DPP) and 2,4-dipyrenylpyrimidine (2,4-DPP).

Briefly, a typical synthesis of 2,4,6-TPP was performed in an air free flask that was charged with 2,4,6-trichloropyrimidine (550mg, 3.0 mmol), pyrenyl-1-boronic acid (2.6657g, 10.8 mmol), and $Pd(PPh_3)_2Cl_2$ catalyst (158 mg, 0.225 mmol) in a glove box. To the reaction vessel, 1,4-dioxane (180 mL, degassed for 60 min with dry nitrogen) and aqueous solution of K_2CO_3 (2.0 M, 75 mL) were introduced while purging with argon. The resultant mixture was stirred at 90 °C for 24 hours under argon atmosphere. The reaction progress was monitored with thin layer chromatography (TLC) and electrospray ionization mass spectroscopy (ESI-MS). After 24 hours, adding ice to the reaction vessel to precipitate brown-green solids, which were filtered, stopped the reaction. The solids obtained were washed several times with brine solution (60 ml × 3) and charged in a column for purification. Pure product was achieved with flash

column chromatography 2:3 hexane: chloroform ($CHCl_3$) for 2,4-DPP, 0.1% MeOH in $CHCl_3$ for 2,5-DPP, 1% MeOH in $CHCl_3$ for 4,6-DPP and finally 1:1 hexane: $CHCl_3$ for TPP. The products obtained from column purification were further dissolved in $CHCl_3$ and recrystallized with MeOH to give yellow and brown solids of the desired compounds with high yields (50-90%). All pyrenyl-pyrimidine compounds obtained were characterized with ESI-MS and nuclear magnetic resonance (NMR) spectroscopy and the spectral details are included in appendix.

2.4. Results and Discussion

2.4.2. Thermal Gravimetric Analysis (TGA) and Melting Point

The ability to withstand high temperature operations and storage is one of the most important reliability-related features of OLEDs desired today. Therefore, the decomposition temperature (T_d) of the pyrenyl-pyrimidine compounds is an important characteristic for long-term operation OLEDs devices. Since OLEDs generate heat as a result of thermionic emission and electrical stress, decomposition of the organic layer often occurs, suggesting that the synthesized blue emitter should be of high thermal stability.[152] Consequently, stability of the pyrenyl-pyrimidine materials upon heating was evaluated using TGA, and results are presented in Figure 2.2. TGA measurements indicate that all pyrenyl-pyrimidine compounds have high thermal stabilities with T_d (corresponding to 5% weight loss) ranging from 420 °C to 550 °C as shown in Table 2.1, which indicates that these compounds have a high potential for their application in OLEDs devices. The T_d for 2,5-DPP and TPP was higher than 2,4-DPP and 4,6-DPP, presenting an advantage from these last two compounds previously reported. It is hypothesized that thermal stabilities were greatly enhanced due to presence of more pyrene moieties in these new compounds in case of the TPP, which leads to an increase in inter and intramolecular interactions thus leading to higher thermal stability. The high thermal stability

observed in TPP could translate not only to high power and brightness operations, but also to applications such as automotive lighting, where the interior automobile temperature often exceeds the ambient temperature by 50 °C or more.[153] Furthermore, high thermal stability will be reflected in high lifetime capabilities due to a lower degradation by temperature over time.[154]

Table 2.1. Summary of the Melting and Thermal Properties of Pyrenyl-Pyrimidines

Compounds	**Melting Point (°C)**	**Decomposition temperature (T_{onset}) (°C)**
2,4-DPP	234	422
4,6-DPP	293	429
2,5-DPP	260	435
TPP	>300	490

All pyrenyl-pyrimidine compounds presented high melting points as shown in Table 2.1 with their melting point ranging from 234 to more than 300 °C. Melting temperatures of pyrenyl-pyrimidines increased in the following order 2,4-DPP, 4,6-DPP, 2,5-DPP and TPP, which paralleled the TGA trend. The melting point trend is attributed to the structure of these pyrenyl-pyrimidine compounds, with TPP having the highest melting point due to enhanced inter- and intramolecular interaction emanating from the additional pyrene ring in the molecule. The high melting point is essential when designing OLEDs emissive materials, as the material needs to withstand high temperature.

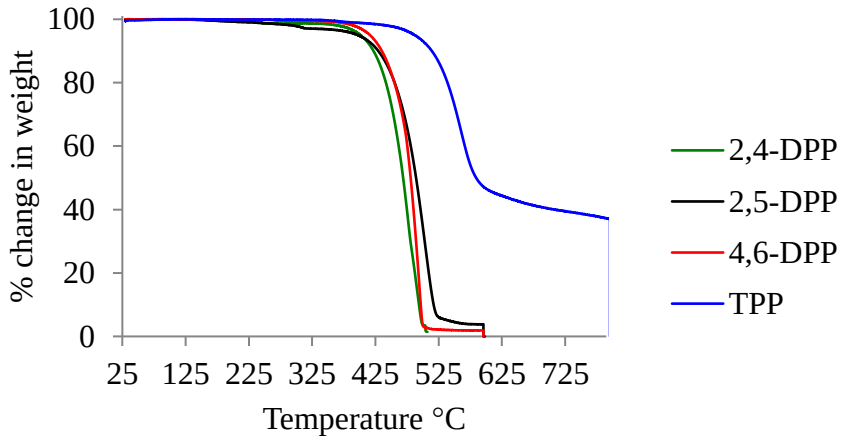

Figure 2.2. Thermogravimetric results for the DPPs and TPP materials synthesized

2.4.3. Powder X-ray diffraction (PXRD)

Extensive research has focused on the design of amorphous materials to avoid nonlinear optical activity from crystalline materials for OLEDs.[155] The solid-state conformation often influences molecular aggregation and thin-film morphology, thus affecting photo-physical properties of chromophoric compounds, particularly in solid phase. Powder X-ray diffraction (PXRD) was therefore employed to estimate the crystalinity and bulky conformations of the synthesized pyrenyl-pyrimidines. With packing difficulties, TPP showed broad peaks with low intensity, which indicated that this compound was amorphous in the solid state (see Figure 2.8 in appendix). While 2,4-DPP, 2,5-DPP and 4,6-DPP showed sharp peaks of low intensity indicating they are semi-crystalline compounds in nature.

The amorphous nature of TPP is attributed to highly twisting conformation adopted by these compounds due to intramolecular steric hindrance caused by connections to the small pyrimidine molecule. The twisted conformation helps to prevent any specific strong intermolecular interactions such as π-π^* stacking as shown in supporting materials (Appendix Figure 2.8). The most important and interesting observation was that, the molecular packing that might be present in the TPP and 2,5-DPP did not alter the fluorescence properties of these compounds, as there was insignificant red shifting of the fluorescence maxima as observed in Figures 2.4 and 2.5. This is important especially for their potential to be employed as materials for OLEDs devices, as the deep blue color associated with these compounds in solid state is not affected since the compounds optical properties lie within the deep blue region.

2.5. Photophysical Properties

2.5.1. UV-Vis Spectroscopy

UV-vis absorption spectra of pyrenyl-pyrimidines were recorded for their dilute chloroform solution (10 μM) and thin films as shown in Figure 2.3. Thin films were formed on quartz slides using spin coating method. Evaluation of the results presented in Figure 2.3 showed that 2,5-DPP and TPP showed three broad absorption bands in both solid and solution state, with absorption peak maxima (A_{max}) at 240 ± 1 nm (A_{max3}), 281 ± 3 nm (A_{max2}), and 376 ± 5 (A_{max1}). Both the solid and solution state absorption spectra resembled that of pure pyrene. The absorption peaks are assigned to S_0 to S_3 (A_{max3}), S_0 to S_2 (A_{max2}) and S_0 to S_1 (A_{max1}) electronic transitions. Due to interchromophore electronic interaction, there was substantial broadening of the absorption bands, which was more pronounced in solid state. The interchromophore interaction could occur as a result of pyrene interaction within the same molecule. Further broadening could be attributed to intermolecular electronic interaction in the solid state.[156] Accordingly, all compounds showed very slight peak shifts in their absorption in solid state, where a 10 nm red shift was observed as is represented in Figure 2.3 and Figure 2.13 of appendix. This shift indicates that pyrene is presumed to be highly twisted around the pyrimidine core, which results in non-coplanar pyrenylpyrimidine moieties that can effectively suppress the intermolecular π-π* stacking in the solid state.[157] Interestingly, in the case of TPP, there was minimal change in the absorption maxima upon its transition to solid state. It can be seen that all of the four compounds in solution showed similar absorption bands at a wavelength of approximately 281 ± 1 nm, which can be attributed to the π-π^* transition of their common pyrene rings.[157] The higher wavelength absorption bands that range from 360 to 370 nm for the solution

and 370 to 380 nm for the solid-state in thin films originates from π to π^* transition from pyrene electron rich ring (donor) to pyrimidine electron deficient ring (acceptor).

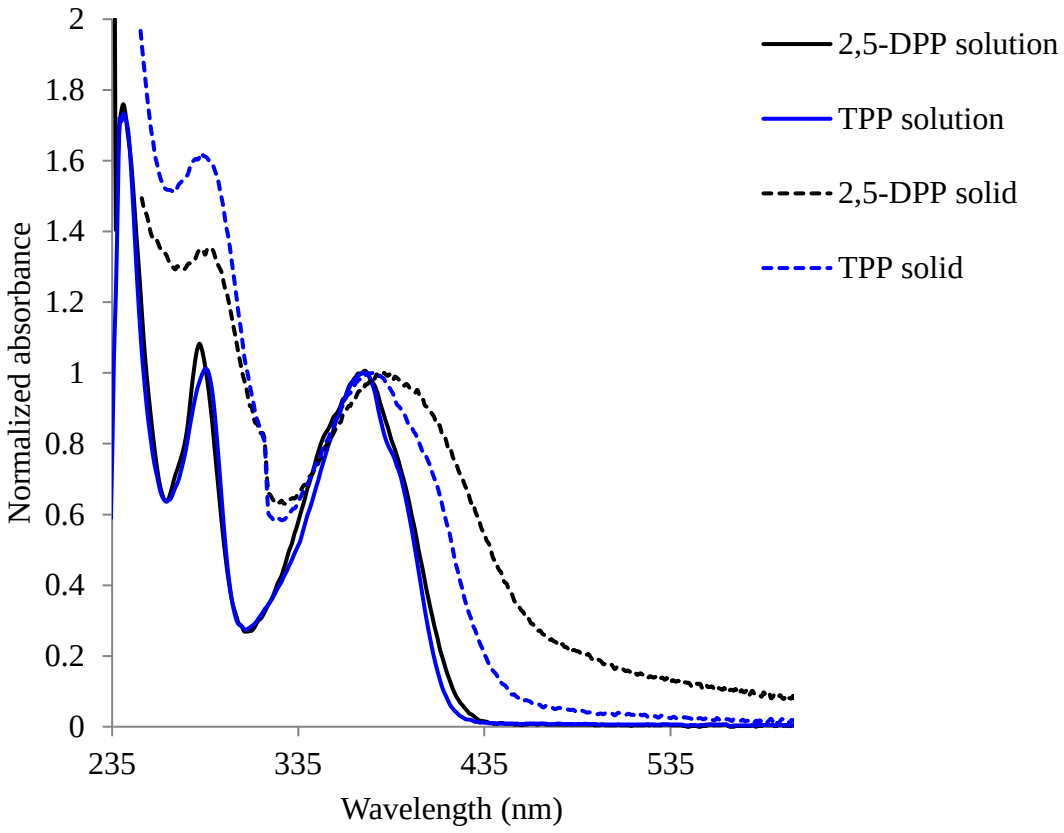

Figure 2.3. Solid lines represent the UV-Vis spectra for normalized 10 μM $CHCl_3$ solution of each DPPs and TPP. Dashed lines represent UV-Vis spectra of solid state of DPPs and TPP spin coated on quartz glass.

The energy band gap (E_{gap}), which is defined as the energy difference between the highest occupied molecular orbital (HOMO) and the lowest unoccupied molecular orbital (LUMO), was calculated from the onset of the lowest energy absorption peak. That is, the negative tangent line of the lowest energy absorption peak that intersects with a linear tangent line of the absorption tail as shown in Figure 2.14 of the appendix section. The energy band gap in most cases indicates the region in which the compound or optoelectronic material emits,

whether blue, red or green region. Energy band gaps varied from 2.5 to 3 eV both in solution and solid state and it was determined as shown in Figure 2.14 of the appendix section and from equation 1. The energy band gaps for the newly synthesized pyrenyl-pyrimidine compounds were observed to be closer to the desired literature value of 2.64 E_v,[158] a value associated with blue emission. Key photophysical data (band gaps) are summarized in Table 2.2

$$E_{Gap} = \frac{1240}{\lambda_{max}} \quad (1)$$

Table 2.2. Band Gap of Synthesized OLEDs Compounds in Solution and Film

Compound	E_{gap} **(eV) Solution (10 μM)**	E_{gap} **(eV) Film (1 mM)**
2,4-DPP	3.05	2.89
4,6-DPP	3.06	2.69
2,5-DPP	2.95	2.58
TPP	2.99	2.82

Molar absorptivity was also determined and is presented in Table 2.3 below. The molar absorptivity for DPPs were very close to the molar absorptivity of pyrene, but for TPP, this value was higher than that of pyrene, which was attributed to the increase in pyrene moieties in this molecule. Since molar absorptivity is a measure of how a compound can efficiently absorb light, TPP shows potent with how it interacts with light. This is interesting because it indicates that more molecules are likely to be promoted to the excited state.

Table2.3. Molar Absorptivity of the DPPs and TPP

Compound	**ε (L mol^{-1} cm^{-1})**
2,4-DPP	59,500
4,6-DPP	52,400
2,5-DPP	48,700
TPP	79,100
Pyrene	54,000

2.5.2. Fluorescence Spectroscopy

Fluorescence spectra of all pyrenyl-pyrimidines were recorded in dilute chloroform (1μM) and in thin films prepared by spin coating. Results are presented in Figures 2.4 and 2.5 below. Emission spectra of all pyrenyl-pyrimidines in dilute solution largely resembled to pyrene emission with spectra maxima in the range of 420-460 nm, although the single band was considerably broadened and showed no fine vibronic structure as shown in Figure 2.4 below.

Analysis of the results presented in supporting information Figure 2.11 (appendix section) showed that 2,5-DPP and TPP presented high fluorescence intensity in solution form. Their fluorescence intensity in solution nearly double in magnitude compared to 2,4-DPP and 4,6-DPP as observed in supporting information Figure 2.11 (appendix section). Interestingly, TPP displayed highest intensity, which is presumably due to three pyrene moieties in its structure.

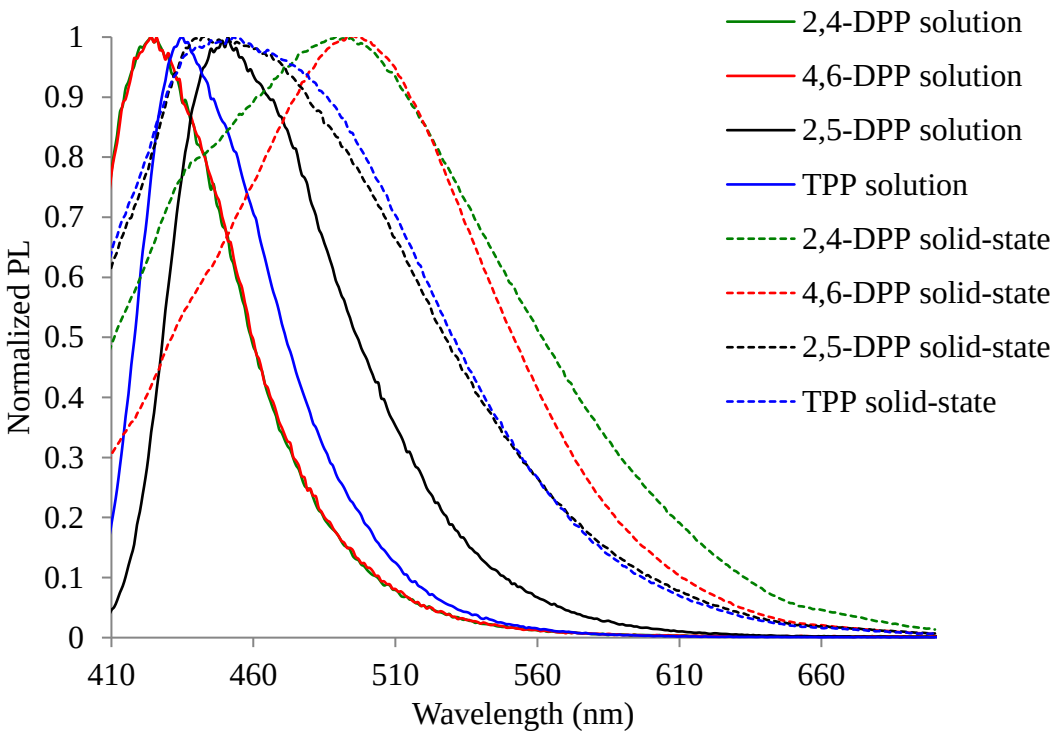

Figure 2.4. Fluorescence emission of 2 μM DPPs and TPP in CHCl3 solution and in solid state.

In thin films, 2,4-DPP and 4,6-DPP recorded higher fluorescence intensities, with 4,6-DPP showing the highest fluorescence intensity as indicated in Figure 2.5. This effect could be attributed to aggregation-enhanced emission associated with 2,4-DPP and 4,6-DPP. Similarly, there was a fluorescence band shift of approximately 50 nm with 2,4-DPP and 4,6-DPP in solid state, which was not seen in the 2,5-DPP and TPP (Figure 2.4). This effect is presumably associated to the structure of the compounds since 2,4-DPP and 4,6-DPP that are possibly more symmetrical than the 2,5-DPP and TPP. This symmetrical structure associated with 2,4-DPP and 4,6-DPP may promote stronger π-π^* stacking which may hinder conformational changes such as rotation, causing an aggregation induced fluorescence enhancement as well as an emission shift of around 50 nm in thin films from solution. This emission shifting could be originating from excimer formation where the two pyrene units are in close proximity such that HOMO of one pyrene unit overlaps with the LUMO of the other pyrene unit to yield the excimer band that is significantly red shifted.[159] 2,5-DPP has the two pyrene molecules on para position, which presumably separates the HOMO and LUMO, causing them to be far from each other; thus, no overlap and no excimer band formation, which leads to insignificant red shifting with 2,5-DPP.

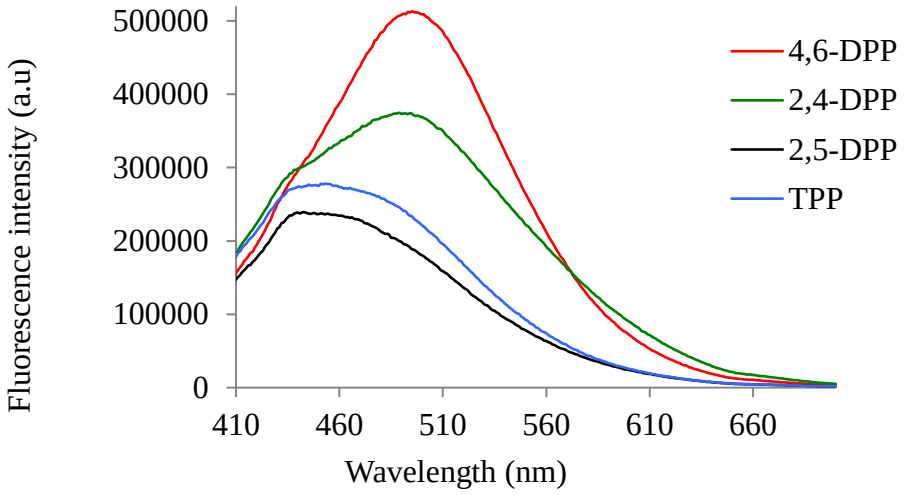

Figure 2.5. Fluorescence emission of DPPs and TPP spin coated thin films

Concentration based fluorescence results are given in supporting information Figure 2.12 (appendix), which shows an aggregation induced enhancement with 2,4-DPP and 4,6-DPP and aggregation induced slight quenching with 2,5-DPP and TPP. The slight quenching observed with the 2,5-DPP and TPP is due to the aggregation of these structures, which leads to a slight change in the intensity. Interestingly, there is no significant change in the band position for 2,5-DPP and TPP thin films. Since the spectral peak positions for 2,5-DPP and TPP are not significantly altered, it was concluded that there is insignificant excimer formation in these solid-state films, while 2,4-DPP and 4,6-DPP's promote their respective excimers' formation, which is an aggregation that induces fluorescence enhancement rather than quenching. The photoluminescence of all the pyrenyl-pyrimidines were approximately confined to blue region of the electromagnetic spectrum (EMS) in dilute solutions and greenish-blue region of the EMS in the solid-state.

Table 2.4. Summary of Emission Properties of Pyrenyl-pyrimidines [a] in Chloroform (2.5μM) While the Films were Spin Coated with 100μM in Chloroform.

Compounds	Absorption Maxima (nm)		Emission Maxima (nm)		Excitation Wavelength (nm)		Stokes Shift (nm)	
	Sol[a]	Film	Sol[a]	Film	Sol[a]	Film	Sol[a]	Film
2,4-DPP	365	374	425	489	375	384	60	115
2,5-DPP	372	381	462	440	382	391	92	59
4,6- DPP	365	377	427	493	375	387	62	116
2,4,6-TPP	370	372	434	454	380	382	64	82

2.6. Quantum yields measurements and Commission Internationale de l'éclairage (CIE)

High photoluminescence efficiency is an important quality to look for good OLED emitters, but is not the only criteria for determining electroluminescence efficiency of OLED emitters. This is because the electroluminescence mechanism of an emitter may be influenced by additional factors that are independent on photoluminescence mechanism; for example,

electroluminescence efficiency is strongly affected by OLED architecture and materials electrical properties.[160, 161] Photoluminescence efficiency of OLEDs emitter is determined in terms of PLQY, defined as the ratio of emitted photons to absorbed photons.[162] For this reason, absolute quantum yield were determined in dilute chloroform solution (2.5μM) and in thin films on quartz glass, for all the DPPs and TPP compounds, using an integrating sphere attached to a spectrofluorometer. Both TPP and 2,5-DPP were observed to have high quantum yield of 80.05% and 105%, respectively. 2,4-DPP and 4,6-DPP measured quantum yields of 46.4% and 41.4% in solution respectively. The high quantum yield observed with 2,5-DPP is presumably due to structure of the molecule, which may promote the generation of two photons upon excitation. To obtain more light from the plane substrate, horizontal orientation of the emitter must be necessary because perfect horizontal orientation can boost EQE up to 45%, which is 1.5 times greater than that for the random orientation.[163] This more rigid planarity presumably results in the inhibition of internal conversion rates and vibrational motions in these compounds in solution form.

From the analysis of photoluminescence spectrum, we were able to calculate the chromaticity coordinates according to the standard established by the CIE (Table 2.3). The pyrenylpyrimidine compounds synthesized showed cyan blue fluorescence in solution while greenish-blue fluorescence in the solid state. From the CIE coordinate calculated, all pyrenyl-pyrimidines were found suitable as blue emitters due to these compounds present CIE coordinates closer to the recommended value for blue emitter of (0.15, 0.06). The y-ordinate of the 2,5-DPP was higher than expected, which explained why the 2,5-DPP gave a sky blue color on illumination with UV. The CIE coordinate however showed that these compounds are indeed blue emitters.

Table 2.5. Summary of quantum yield and C.I.E Properties of Pyrenyl-pyrimidines [a] in Chloroform (2.5μM) While the Films were Spin Coated with 100μM in Chloroform.

Compounds	PLQY (%)		CIE Coordinates (x,y)
	Sol[a]	Film	Sol[a]
2,4-DPP	46.35	46.78	0.16, 0.05
2,5-DPP	105	65.32	0.16, 0.14
4,6- DPP	41.37	44.34	0.16, 0.05
2,4,6-TPP	80.05	1.74	0.15, 0.07

Because the pyrenyl-pyrimidine compounds encompass both the electron donating (pyrene) and electron withdrawing (pyrimidine) moieties in the same molecule, this potential could lead to the formation of the intramolecular charge transfer (ICT) states, which means the material acts both as a hole and electron transport material. The formation of ICT states could, in principle, lead to undesirable changes in spectral characteristics such as bathochromic shift witnessed with 2,4-DPP and 4,6-DPP, broadening of the spectra bands quenching or enhancement of the fluorescence intensity, decrease in the quantum efficiency among other changes. In our studies, the formation of ICT was investigated from the solvatochromic studies of the pyrenylpyrimidines. Photoluminescence spectra of these compounds were recorded in solvent of varying polarity from hexane to DMSO as indicated in Figure 2.14. The emission band maxima of all the compounds red shifted with increasing solvent polarity from 394 ± 2nm (Hexane) to 463 ± 2nm (DMSO), suggesting the possibility of some charge transfer participation in photoluminescence spectra. Furthermore, there was considerable decrease in the fluorescence intensity with increase in polarity for all the pyrenyl-pyrimidines (Figure 2.14 in appendix section), which further suggested the possibility of the charge transfer from the fluorescence pyrene moiety to non-fluorescence pyrimidine electron acceptor.

2.7. Photostability Measurements

Photostability and thermal stability are extremely important properties for development of OLED devices. An emitting material with significantly high photo- and thermal stability would enhance the overall lifetime as well as the applications of such materials under a variety of conditions. Analysis of the data presented in Figure 2.7 shows that 2,5-DPP and TPP are relatively photostable compared to their isomeric counterparts, 2,4-DPP and 4,6-DPP. The high photostabilities for 2,5-DPP and TPP are due to high degree of inter- and intramolecular forces that may possibly be emanating from the hydrogen bonding of the hydrogen atoms of the pyrene moieties with the nitrogen atoms of the neighboring molecules, which has been shown to increase photostabilities.[164] This is an advantage for the two novel structures and their potential application for OLEDs devices because they are required to be highly stable both thermally and upon prolonged exposure to light. Interestingly, 2,5-DPP, which is the most promising deep blue emitter, from the CIE coordinates data obtained in solution form and insignificance change on fluorescence spectra upon fabricating the solid films, showed insignificant change upon photo illumination at very strong laser beam.

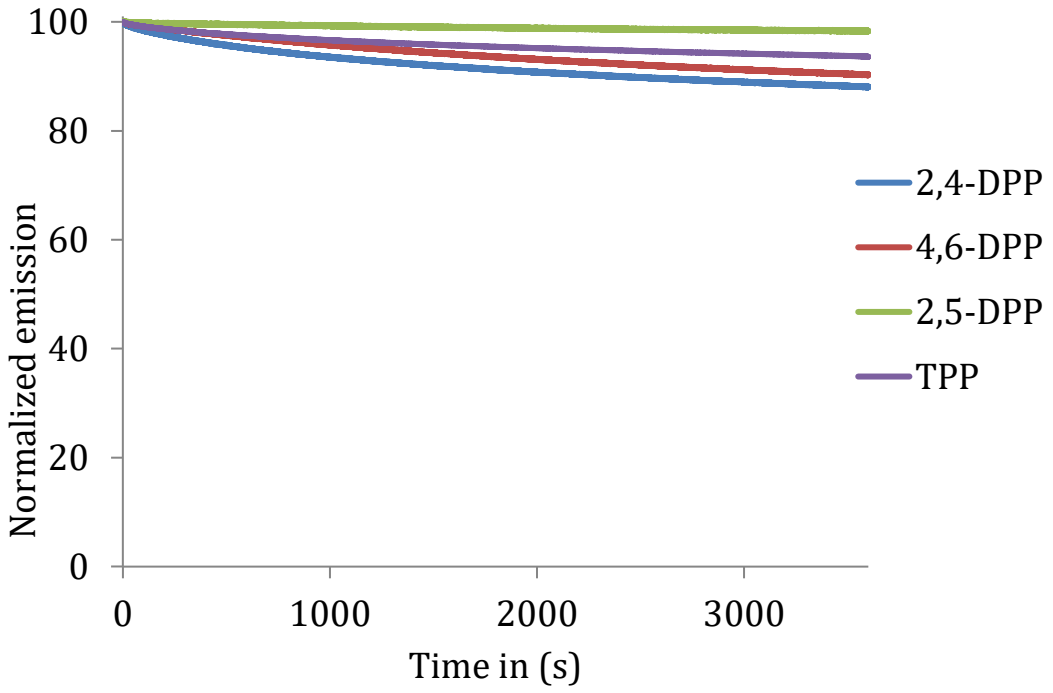

Figure 2.6. Photostability of DPPs and TPP in solid state.

2.8. Conclusion and Future Work

In summary, we have designed and synthesized pyrimidine-based materials with a donor-π-acceptor structure by attaching strong electron-donating moiety of pyrenes to different positions of the strong electron acceptor pyrimidine and investigating their potential as non-doped blue emitter materials for OLEDs application. The newly reported 2,5-DPP and TPP fluorophores show high quantum efficiency with 2,5-DPP having a quantum efficiency of greater than 100% and good thermal stability. Evaluation of the spectral properties and calculated band gaps, suggest the potential use of these compounds for optoelectronic applications and as emitting material to be used in OLEDs devices. Furthermore, concentration dependent and fabrication of solid-state films indicated insignificant fluorescence intensity decrease for 2,5-DPP and TPP, implying suppression of the excimer formation in these newly synthesized

compounds. These molecules also showed high photostability, which is essential for long life required for blue emitters.

For the future work, we propose the measuring of the thickness of the films and the fabrication of the actual device so that the external quantum efficiency (EQE) which is a vital property for the OLEDS may be determined.

APPENDIX. SUPPORTING INFORMATION FOR CHAPTER 2

Synthesis procedure for 2,4-DPP

A mixture of pyrene-1-boronic acid (7.20 mmol, 1771.7 mg), 2,4-dichloropyrimidine (3.0 mmol, 447 mg, Bis(triphenylphosphine)palladium chloride (0.15 mmol, 105 mg) and potassium carbonate solution (2000 mmol, 50 ml) in 1,4-dioxane (120 ml) were stirred at 90 °C for 24 hrs under nitrogen atmosphere. After cooling to room temperature, the mixture was poured into iced water, and the solid formed was filtered, the solids were washed several times with 300 ml brine solution and dried. Solids were then purified by silica gel chromatography with 60% chloroform in hexane. The crude product from the column was further purified by dissolving in chloroform and recrystallizing in methanol several times to obtain more than 85% yield of greenish yellow solids.

2,4-DPP- MS, ESI ($CHCl_3$)- m/z 481.17 ($M+H^+$); ^{1}H NMR ($CDCl_3$, 500 MHz, ppm): δ 9.29 (d, J = 9.30 Hz, 1H), 9.20 (d, J = 4.90 Hz, 1H), 8.85 (d, J = 8.00 Hz, 1H), 8.72 (d, J = 9.25 Hz 1H), 8.41 (d, J = 7.85 Hz 1H), 8.34 (dd, J = 7.85 Hz, 2H), 8.28-8.15(m, 9H), 8.09-8.02(m, 2H), 7.82 (d, J = 5.0Hz, 2H); ^{13}C Proton Decoupled NMR ($CDCl_3$, 125 MHz, ppm): δ 167.69, 167.12, 157.20, 133.09, 133.05, 132.58, 132.44, 131.32, 130.81, 130.79, 129.56, 129.05, 128.80, 128.72, 128.66, 128.47, 128.42, 127.70, 127.43, 127.33, 126.27, 125.99, 125.86, 125.57, 125.55, 125.36, 125.32, 125.25, 125.10, 124.96, 124.85, 124.76, 124.71, 124.31, 119.87.

Synthesis procedure for 4,6-DPP

A mixture of pyrene-1-boronic acid (7.20 mmol, 1771.7 mg), 4,6-dichloropyrimidine (3.0 mmol, 447 mg, Bis(triphenylphosphine)palladium chloride (0.15 mmol, 105 mg) and potassium carbonate solution (2000 mmol, 50 ml) in 1,4-dioxane (120 ml) were stirred at 90 °C for 24 hrs

under nitrogen atmosphere. After cooling to room temperature, the mixture was pored into iced water and the solid formed was filtered, the solids were washed several times with 300 ml brine solution and dried. The solid were then purified by silica gel chromatography with 60% chloroform in hexane. The crude product from the column was further purified by dissolving in chloroform and recrystallizing in methanol several times to obtain more than 85% yield brownish yellow solids.

4,6-DPP- MS, ESI ($CHCl_3$)- m/z 481.17 ($M+H^+$); ^1H NMR ($CDCl_3$, 500 MHz, ppm): δ 9.73 (d, J = 1.0 Hz, 1H), 8.71 (d, J = 9.20 Hz, 2H), 8.35 (dd, J = 13.65, Hz, 4H), 8.27 (t, J = 14.25 Hz, 5H), 8.22-8.15(m, 6H), 8.08 (t, J = 7.58 Hz, 2H); ^{13}C Proton Decoupled NMR ($CDCl_3$, 125 MHz, ppm): δ 167.06, 159.12, 132.82, 132.54, 131.34, 130.81, 128.93, 128.83, 128.79, 127.66, 127.34, 126.35, 125.96,125.65, 125.16, 125.00, 124.71, 124.16, 123.92

Synthesis procedure for 2,5-DPP

A mixture of pyrene-1-boronic acid (7.20 mmol, 1771.7 mg), 2,5-dichloropyrimidine (3.0 mmol, 447 mg, Bis(triphenylphosphine)palladium chloride (0.15 mmol, 105 mg) and potassium carbonate solution (2000 mmol, 50 ml) in 1,4-dioxane (120 ml) were stirred at 90 °C for 24 hrs under nitrogen atmosphere. After cooling to room temperature, the mixture was pored into iced water and the solid formed was filtered, the solids were washed several times with 300 ml brine solution and dried. The solid were then purified by silica gel chromatography with 60% chloroform in hexane. The crude product from the column was further purified by dissolving in chloroform and recrystallizing in methanol several times to obtain more than 85 yield yellow solids.

2,5-DPP- MS, ESI ($CHCl_3$)- m/z 481.17 ($M+H^+$); ^1H NMR ($CDCl_3$, 400 MHz, ppm): δ 9.34 (s, 2H), 9.30 (d, J = 9.4 Hz, 1H), 8.83 (d, J = 8.0 Hz, 1H), 8.38 (dd, J = 7.94 Hz 2H), 8.31-8.17(m, 11H), 8.13 (dd, J = 7.82 Hz, 2H), 8.10-8.06(m, 1H); ^{13}C Proton Decoupled NMR ($CDCl_3$, 125 MHz, ppm): δ 158.03, 132.72, 132.49, 131.80, 131.46, 131.38, 130.90, 130.87, 129.76, 1229.57, 129.00, 128.82, 128.65, 128.62, 128.42, 127.63, 127.49, 127.35, 126.48, 126.12, 125.87, 125.73, 125.52, 125.47, 125.34, 125.23, 125.11, 124.94, 124.81, 124.76, 123.82

Synthesis procedure for 2,4,6-TPP

A mixture of pyrene-1-boronic acid (10.8 mmol, 2657.56 mg), 4,6-dichloropyrimidine (3.0 mmol, 550.26 mg, Bis(triphenylphosphine)palladium chloride (0.225 mmol, 158mg) and potassium carbonate solution (2000 mmol, 75 ml) in 1,4-dioxane (180 ml) were stirred at 90 °C for 24 hrs under nitrogen atmosphere. After cooling to room temperature, the mixture was pored into iced water and the solid formed was filtered, the solids were washed several times with 300 ml brine solution and dried. The solid were then purified by silica gel chromatography with 60% chloroform in hexane. The crude product from the column was further purified by dissolving in chloroform and recrystallizing in methanol several times to obtain more than 50% yield Brownish yellow solids.

TPP- MS, ESI ($CHCl_3$)- m/z 681.32 ($M+H^+$); ^1H NMR ($CDCl_3$, 400 MHz, ppm): δ 9.60 (d, J = 9.4 Hz 1H), 9.09 (d, J = 8.04 Hz, 1H), 8.92 (d, 2H), 8.57 (d, J = 7.88 Hz, 2H), 8.39(t, J = 8.34 Hz, 3H), 8.30-8.17 (m, J = 7.82 Hz, 15H), 8.10(dd, J = 7.34 Hz, 3H) 8.07- 8.02 (m, 1H); ^{13}C Proton Decoupled NMR ($CDCl_3$, 125 MHz, ppm): δ 167.16, 133.46, 132.65, 132.46, 131.35, 130.84, 129.34, 128.96, 128.76, 128.66, 128.46, 128.37, 127.85, 127.47, 127.36, 126.28, 125.95, 125.85, 125.76, 125.56, 125.29, 125.17, 125.03, 124.90, 124.76, 124.51, 121.15

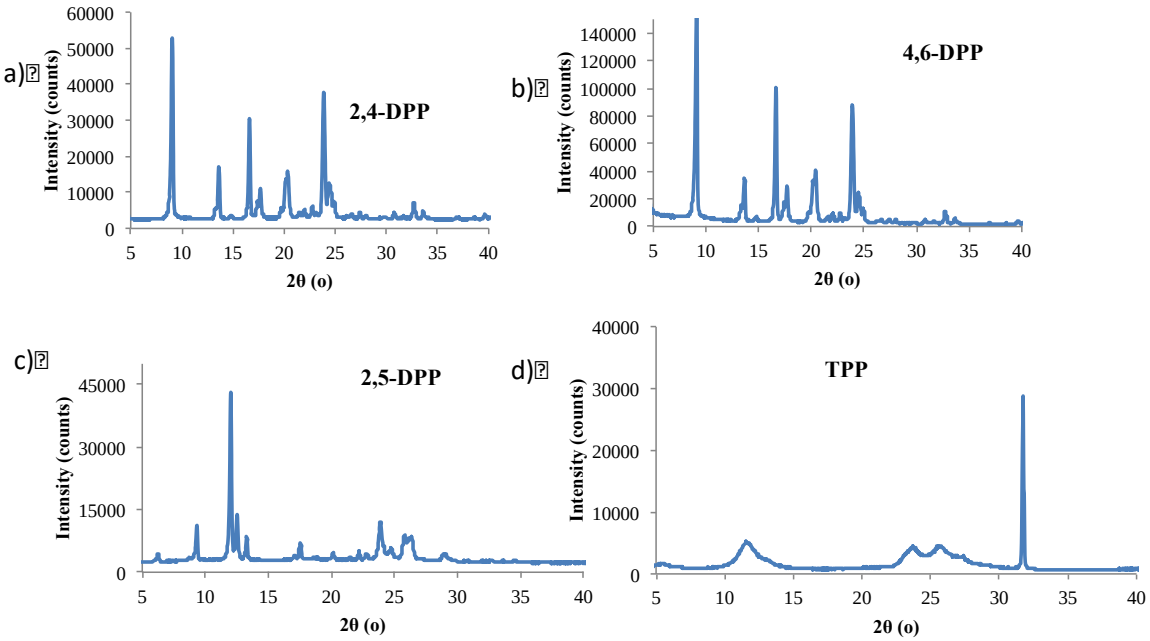

Figure 2.7. The XRD for (a) 2,4-DPP, (b) 4,6-DPP, (c) 2,5-DPP and (d) TPP

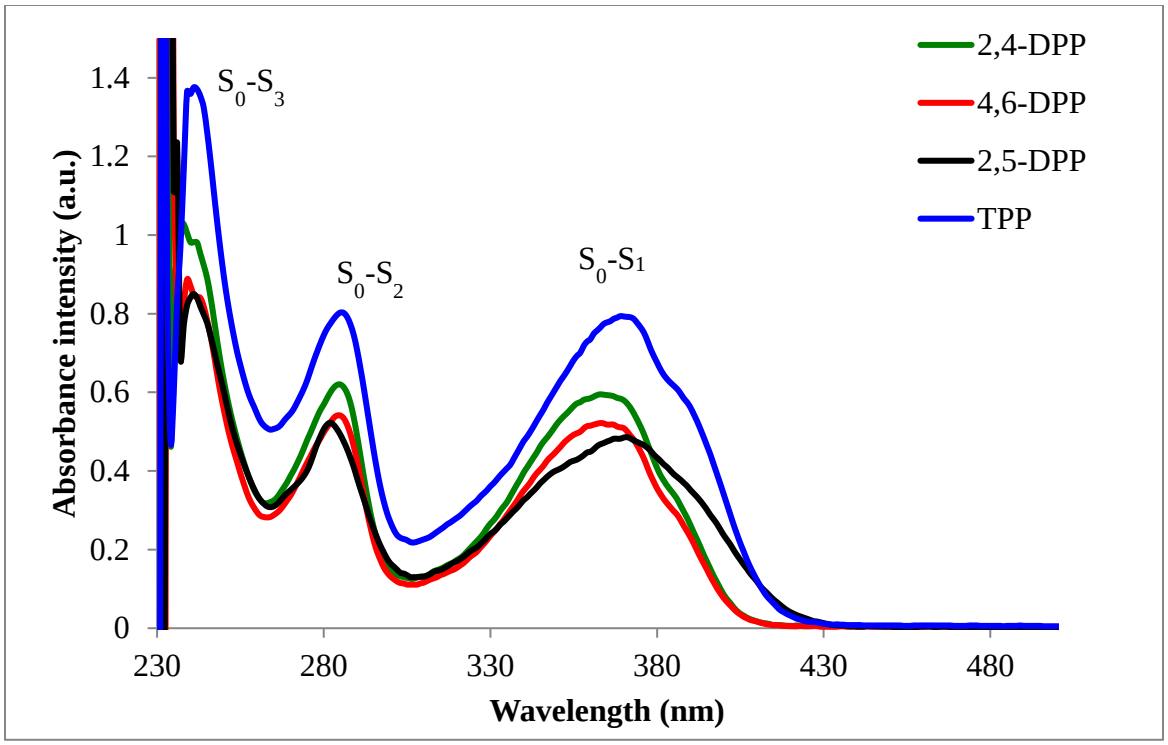

Figure 2.8. UV-Vis spectra for 10 μM of DPPs and TPP in $CHCl_3$

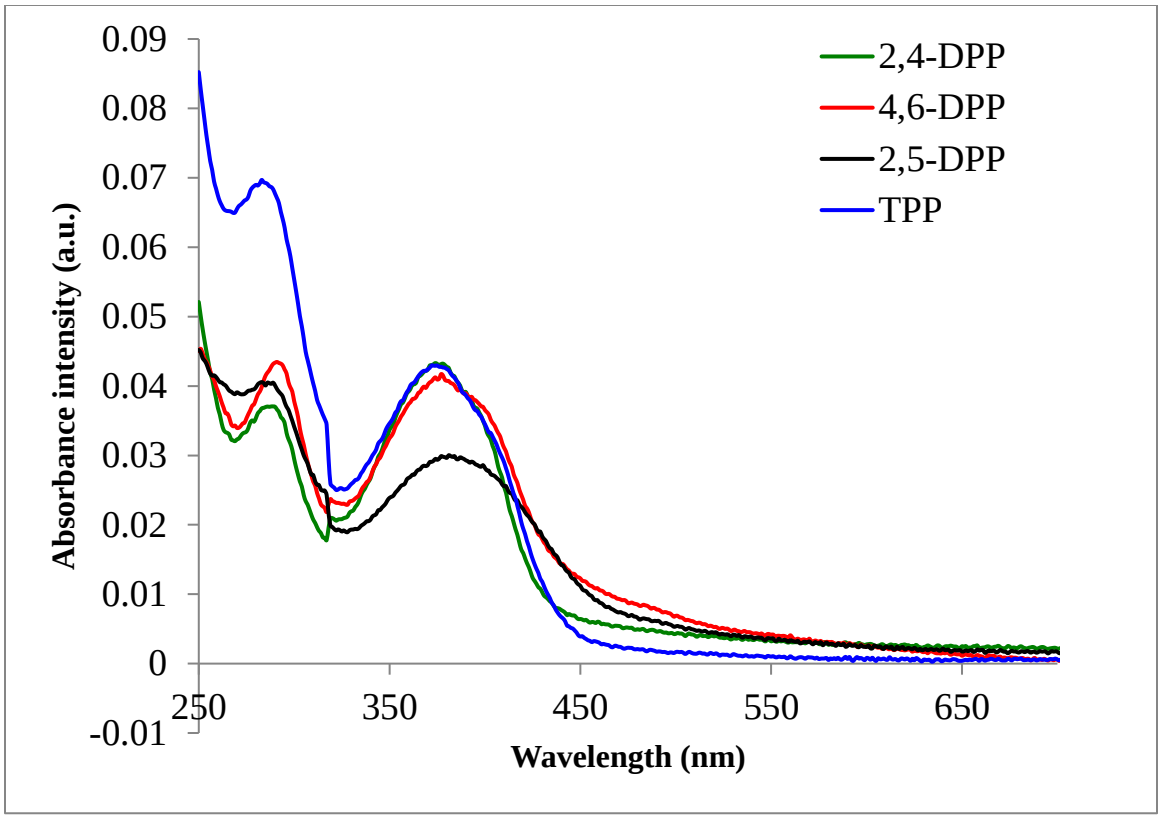

Figure 2.9. UV-Vis spectra of DPPs and TPP samples (in $CHCl_3$) in solid state

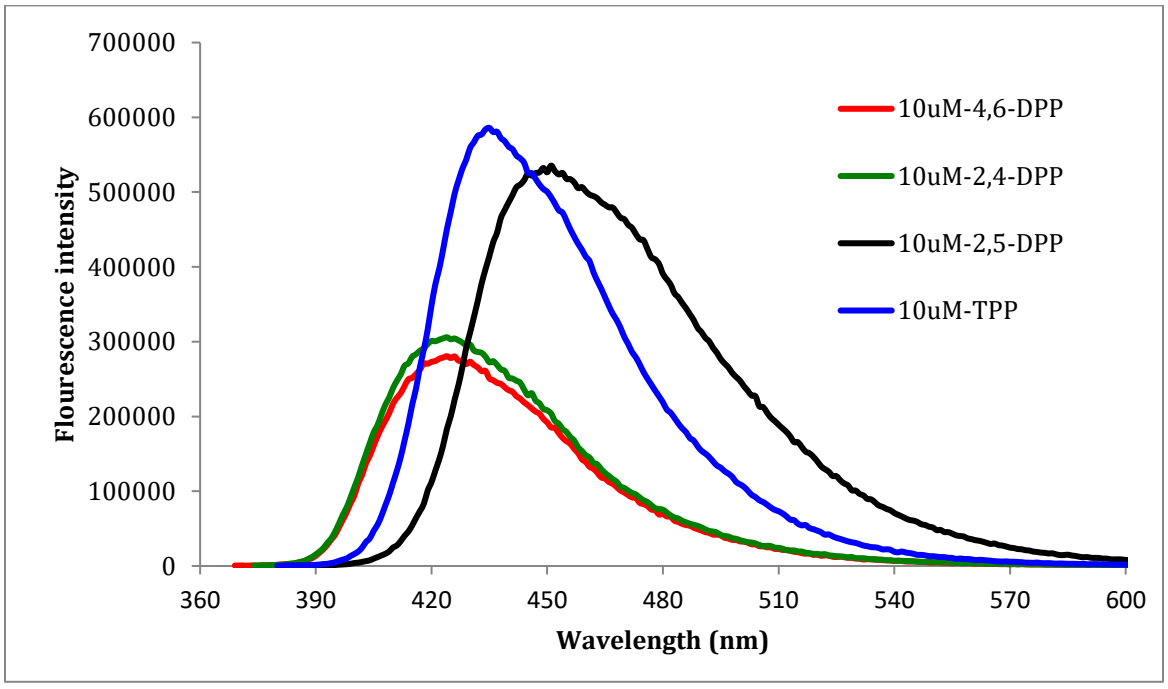

Figure 2.10. Fluorescence spectra for 10μM of 4,6- and 2,4-DPPs in $CHCl_3$

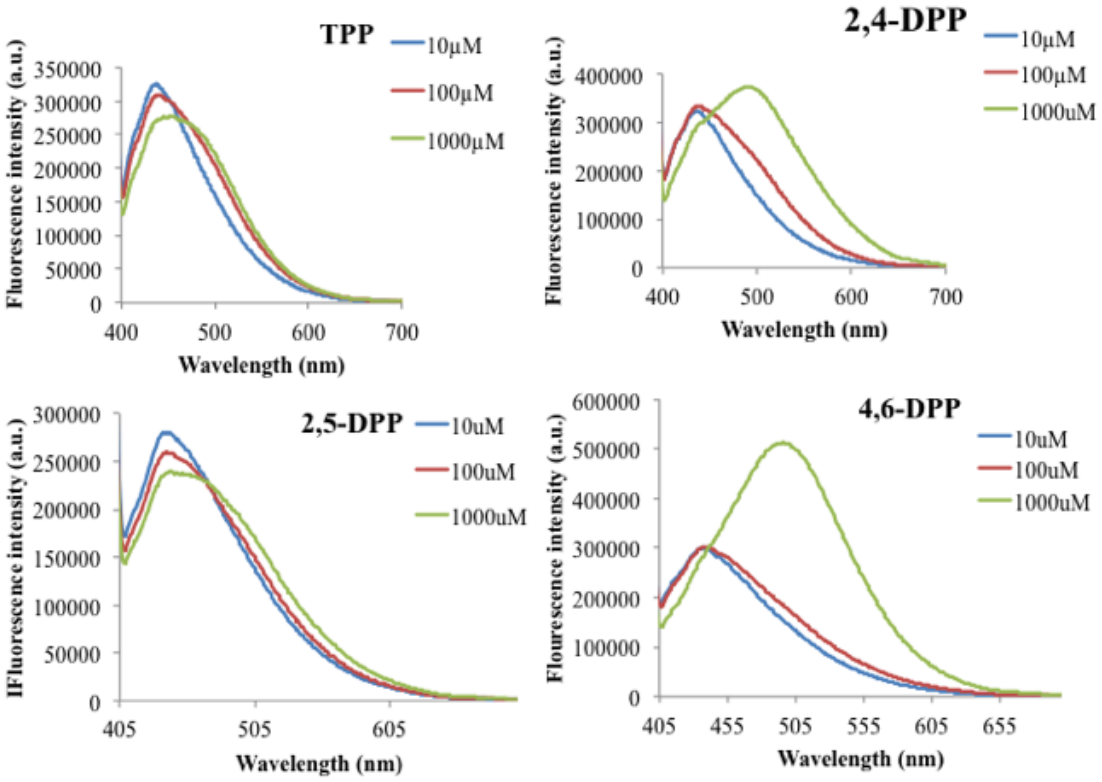

Figure 2.11. Concentration dependent fluorescence data

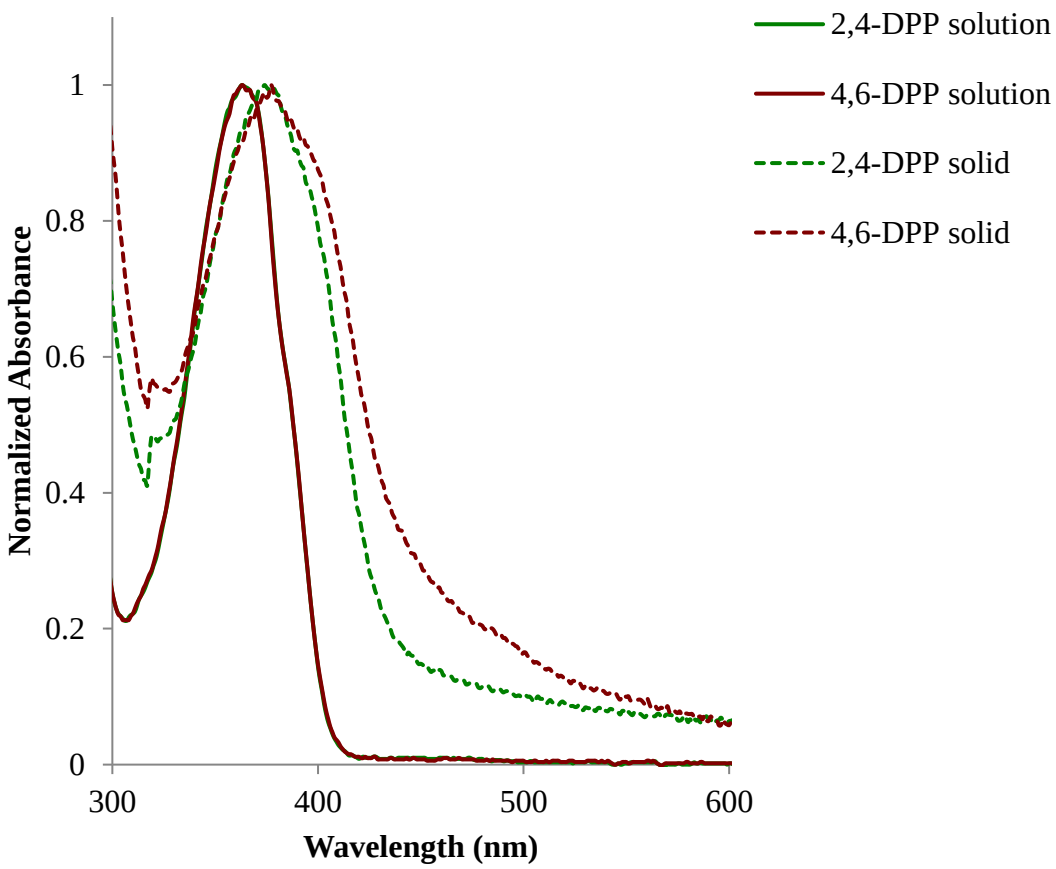

Figure 2.12. Fluorescence spectra for 10μM of DPPs and TPP in $CHCl_3$

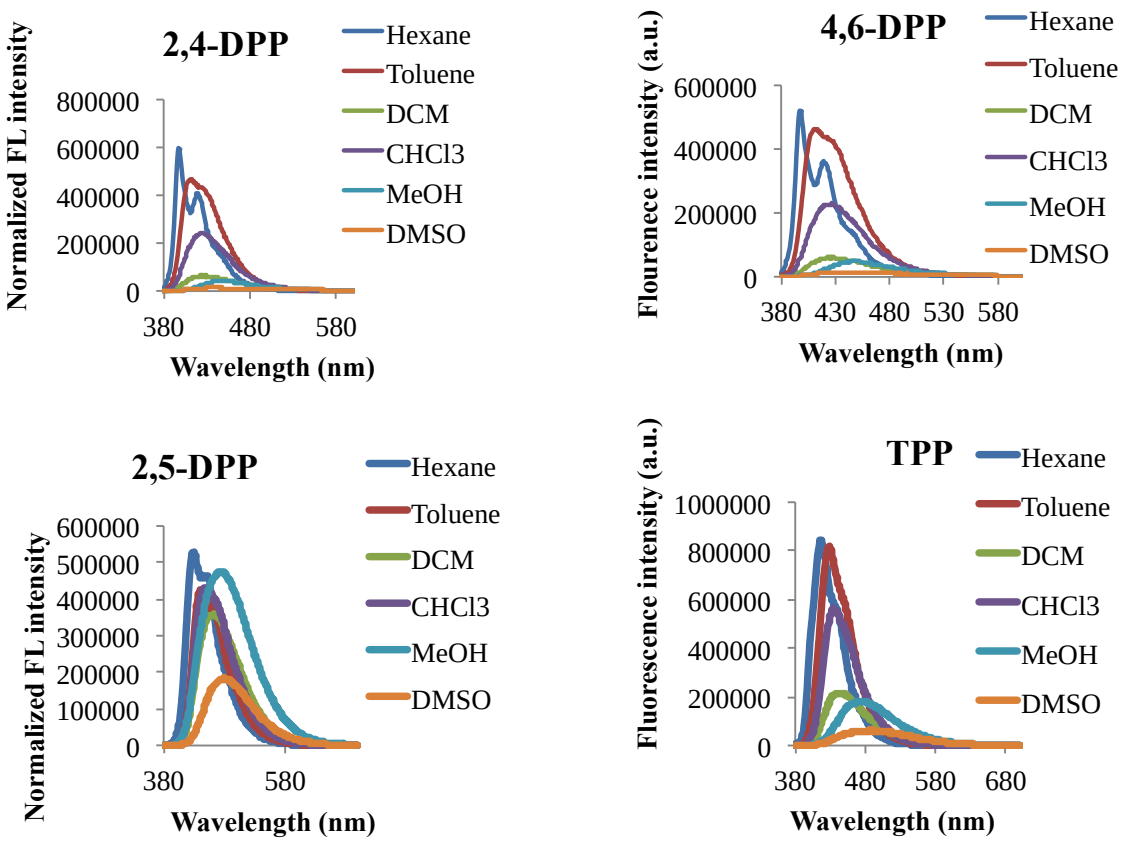

Figure 2.13. Solvatochromic effect for the neutral pyrenylpyrimidines

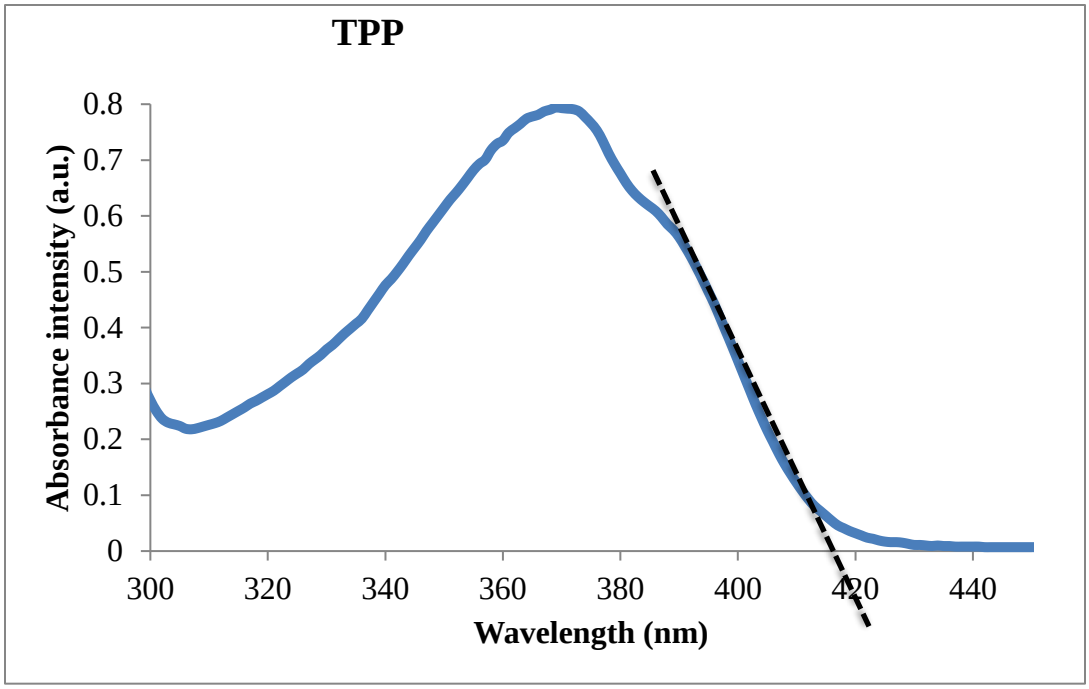

Figure 2.14. Determination of the band gap from absorption data of TPP

REFERENCES

1. Kaplunov, M. G.; Yakushchenko, I. K.; Krasnikova, S. S.; Echmaev, S. B., Novel 1, 8-bis (diarylamino) pyrenes as OLED materials. *Mendeleev Communications* **2016,** *5* (26), 437-439.

2. Horowitz, G., Organic semiconductors for new electronic devices. *Advanced Materials* **1990,** *2* (6-7), 287-292.

3. Stolterfoht, M.; Armin, A.; Philippa, B.; White, R. D.; Burn, P. L.; Meredith, P.; Juška, G.; Pivrikas, A., Photocarrier drift distance in organic solar cells and photodetectors. *Scientific reports* **2015,** *5*, 9949.

4. Shaw, J. M.; Seidler, P. F., Organic electronics: introduction. *IBM Journal of Research and Development* **2001,** *45* (1), 3-9.

5. Müllen, K.; Scherf, U., *Organic light emitting devices: synthesis, properties and applications*. John Wiley & Sons: 2006.

6. So, F.; Kido, J.; Burrows, P., Organic light-emitting devices for solid-state lighting. *MRS bulletin* **2008,** *33* (7), 663-669.

7. Sasabe, H.; Kido, J., Development of high performance OLEDs for general lighting. *Journal of Materials Chemistry C* **2013,** *1* (9), 1699-1707.

8. Islam, A.; Rabbani, M.; Bappy, M. H.; Miah, M. A. R.; Sakib, N. In *A review on fabrication process of organic light emitting diodes*, 2013 International Conference on Informatics, Electronics and Vision (ICIEV), IEEE: 2013; pp 1-5.

9. Park, J.-S.; Chae, H.; Chung, H. K.; Lee, S. I., Thin film encapsulation for flexible AM-OLED: a review. *Semiconductor science and technology* **2011,** *26* (3), 034001.

10. Nakanotani, H.; Higuchi, T.; Furukawa, T.; Masui, K.; Morimoto, K.; Numata, M.; Tanaka, H.; Sagara, Y.; Yasuda, T.; Adachi, C., High-efficiency organic light-emitting diodes with fluorescent emitters. *Nature communications* **2014,** *5*, 4016.

11. Moliton, A.; Hiorns, R. C., Review of electronic and optical properties of semiconducting π-conjugated polymers: applications in optoelectronics. *Polymer International* **2004,** *53* (10), 1397-1412.

12. Li, B.; Li, Z.; Hu, T.; Zhang, Y.; Wang, Y.; Yi, Y.; Guo, F.; Zhao, L., Highly efficient blue organic light-emitting diodes from pyrimidine-based thermally activated delayed fluorescence emitters. *Journal of Materials Chemistry C* **2018,** *6* (9), 2351-2359.

13. Zhu, Z.-L.; Chen, M.; Chen, W.-C.; Ni, S.-F.; Peng, Y.-Y.; Zhang, C.; Tong, Q.-X.; Lu, F.; Lee, C.-S., Removing shortcomings of linear molecules to develop high efficiencies deep-blue organic electroluminescent materials. *Organic Electronics* **2016,** *38*, 323-329.

14. Antoniadis, H., Overview of OLED display technology. *cell* **2003,** *408*, 314-6460.

15. Dailey, S.; Feast, W. J.; Peace, R. J.; Sage, I. C.; Till, S.; Wood, E. L., Synthesis and device characterisation of side-chain polymer electron transport materials for organic semiconductor applications. *Journal of Materials Chemistry* **2001,** *11* (9), 2238-2243.

16. Kroon, R.; Mengistie, D. A.; Kiefer, D.; Hynynen, J.; Ryan, J. D.; Yu, L.; Müller, C., Thermoelectric plastics: from design to synthesis, processing and structure–property relationships. *Chemical Society Reviews* **2016,** *45* (22), 6147-6164.

17. Shirakawa, H.; Louis, E. J.; MacDiarmid, A. G.; Chiang, C. K.; Heeger, A. J., Synthesis of electrically conducting organic polymers: halogen derivatives of polyacetylene,(CH) x. *Journal of the Chemical Society, Chemical Communications* **1977,** (16), 578-580.

18. Chiang, C. K.; Fincher Jr, C.; Park, Y. W.; Heeger, A. J.; Shirakawa, H.; Louis, E. J.; Gau, S. C.; MacDiarmid, A. G., Electrical conductivity in doped polyacetylene. *Physical review letters* **1977,** *39* (17), 1098.

19. Juhari, N.; Majid, W. H. A.; Ibrahim, Z. A. In *Degradation of single layer MEH-PPV organic light emitting diode (OLED)*, 2006 IEEE International Conference on Semiconductor Electronics, IEEE: 2006; pp 112-115.

20. Han, D.; Khan, Y.; Ting, J.; King, S. M.; Yaacobi-Gross, N.; Humphries, M. J.; Newsome, C. J.; Arias, A. C., Flexible Blade-Coated Multicolor Polymer Light-Emitting Diodes for Optoelectronic Sensors. *Advanced Materials* **2017,** *29* (22), 1606206.

21. Sprengard, R.; Bonrad, K.; Daeubler, T. K.; Frank, T.; Hagemann, V.; Köhler, I.; Pommerehne, J.; Ottermann, C. R.; Voges, F.; Vingerling, B. In *OLED devices for signage applications: a review of recent advances and remaining challenges*, Organic Light-Emitting Materials and Devices VIII, International Society for Optics and Photonics: 2004; pp 173-183.

22. Lu, W.; Kuwabara, J.; Iijima, T.; Higashimura, H.; Hayashi, H.; Kanbara, T., Synthesis of π-conjugated polymers containing fluorinated arylene units via direct arylation: Efficient synthetic method of materials for OLEDs. *Macromolecules* **2012,** *45* (10), 4128-4133.

23. Tang, C. W.; Chen, C. H.; Goswami, R., Electroluminescent device with modified thin film luminescent zone. Google Patents: 1988.

24. Baldo, M.; Kozlov, V.; Burrows, P.; Forrest, S.; Ban, V.; Koene, B.; Thompson, M., Low pressure organic vapor phase deposition of small molecular weight organic light emitting device structures. *Applied physics letters* **1997,** *71* (21), 3033-3035.

25. Karzazi, Y., Organic light emitting diodes: Devices and applications. *J. Mater. Environ. Sci* **2014,** *5* (1), 1-12.

26. Jou, J.-H.; Kumar, S.; Agrawal, A.; Li, T.-H.; Sahoo, S., Approaches for fabricating high efficiency organic light emitting diodes. *Journal of Materials Chemistry C* **2015,** *3* (13), 2974-3002.

27. Lee, K.-H.; Han, C.-Y.; Kang, H.-D.; Ko, H.; Lee, C.; Lee, J.; Myoung, N.; Yim, S.-Y.; Yang, H., Highly efficient, color-reproducible full-color electroluminescent devices based on red/green/blue quantum dot-mixed multilayer. *ACS nano* **2015,** *9* (11), 10941-10949.

28. Salehi, A.; Dong, C.; Shin, D.-H.; Zhu, L.; Papa, C.; Bui, A. T.; Castellano, F. N.; So, F., Realization of high-efficiency fluorescent organic light-emitting diodes with low driving voltage. *Nature communications* **2019,** *10* (1), 2305.

29. Xiao, L.; Su, S. J.; Agata, Y.; Lan, H.; Kido, J., Nearly 100% internal quantum efficiency in an organic Blue-Light electrophosphorescent device using a weak electron transporting material with a wide energy gap. *Advanced Materials* **2009,** *21* (12), 1271-1274.

30. Ahmed, E.; Earmme, T.; Jenekhe, S. A., New solution-processable electron transport materials for highly efficient blue phosphorescent OLEDs. *Advanced Functional Materials* **2011,** *21* (20), 3889-3899.

31. Kido, J. In *61.1: Invited Paper: High Performance OLEDs for Displays and General Lighting*, SID Symposium Digest of Technical Papers, Wiley Online Library: 2008; pp 931-932.

32. Valchanov, G.; Ivanova, A.; Tadjer, A.; Chercka, D.; Baumgarten, M., Tuning the optical absorption of potential blue emitters. *Organic Electronics* **2013,** *14* (11), 2727-2736.

33. Bi, X.; Zuo, W.; Liu, Y.; Zhang, Z.; Zeng, C.; Xu, S.; Cao, S., Organic solution-processible electroluminescent molecular glasses for non-doped standard red OLEDs with electrically stable chromaticity. *Materials Research Bulletin* **2015,** *70*, 865-875.

34. Thejokalyani, N.; Dhoble, S., Novel approaches for energy efficient solid state lighting by RGB organic light emitting diodes–A review. *Renewable and Sustainable Energy Reviews* **2014,** *32*, 448-467.

35. Shinde, D., Design, synthesis and evaluation of solution processable small organic molecules for applications in organic electronics. **2018**.

36. Fernandez-Mato, A.; Quintela, J. M.; Peinador, C., Novel naphthyridine-based compounds in small molecular non-doped OLEDs: synthesis, properties and their versatile applications for organic light-emitting diodes. *New Journal of Chemistry* **2012,** *36* (8), 1634-1640.

37. Zhu, M.; Ye, T.; Li, C.-G.; Cao, X.; Zhong, C.; Ma, D.; Qin, J.; Yang, C., Efficient solution-processed nondoped deep-blue organic light-emitting diodes based on fluorene-bridged anthracene derivatives appended with charge transport moieties. *The Journal of Physical Chemistry C* **2011,** *115* (36), 17965-17972.

38. Tagare, J.; Vaidyanathan, S., Recent development of phenanthroimidazole-based fluorophores for blue organic light-emitting diodes (OLEDs): an overview. *Journal of Materials Chemistry C* **2018,** *6* (38), 10138-10173.

39. Shih, P. I.; Chuang, C. Y.; Chien, C. H.; Diau, E. G.; Shu, C. F., Highly efficient non-doped blue-light-emitting diodes based on an anthrancene derivative end-capped with tetraphenylethylene groups. *Advanced Functional Materials* **2007,** *17* (16), 3141-3146.

40. Shih, P. I.; Chuang, C. Y.; Chien, C. H.; Diau, E. G.; Shu, C. F., Highly efficient non-doped blue-light-emitting diodes based on an anthrancene derivative end-capped with tetraphenylethylene groups. *Advanced Functional Materials* **2007,** *17* (16), 3141-3146.

41. Zhu, M.; Yang, C., Blue fluorescent emitters: design tactics and applications in organic light-emitting diodes. *Chem. Soc. Rev.* **2013,** *42* (12), 4963-4976.

42. Jiang, H.; JunHua, W.; Wei, H., Progress in long wavelength emission in fluorene-based electroluminescent blue materials. *Science in China Series B: Chemistry* **2008,** *51* (6), 497-520.

43. Tsai, T.-C.; Hung, W.-Y.; Chi, L.-C.; Wong, K.-T.; Hsieh, C.-C.; Chou, P.-T., A new ambipolar blue emitter for NTSC standard blue organic light-emitting device. *Organic Electronics* **2009,** *10* (1), 158-162.

44. Hung, W.-Y.; Chi, L.-C.; Chen, W.-J.; Chen, Y.-M.; Chou, S.-H.; Wong, K.-T., A new benzimidazole/carbazole hybrid bipolar material for highly efficient deep-blue electrofluorescence, yellow–green electrophosphorescence, and two-color-based white OLEDs. *Journal of Materials Chemistry* **2010,** *20* (45), 10113-10119.

45. Zassowski, P.; Ledwon, P.; Kurowska, A.; Herman, A. P.; Lapkowski, M.; Cherpak, V.; Hotra, Z.; Turyk, P.; Ivaniuk, K.; Stakhira, P.; Sych, G.; Volyniuk, D.; Grazulevicius, J. V., 1,3,5-Triazine and carbazole derivatives for OLED applications. *Dyes and Pigments* **2018,** *149*, 804-811.

46. Salunke, J. K.; Wong, F. L.; Feron, K.; Manzhos, S.; Lo, M. F.; Shinde, D.; Patil, A.; Lee, C. S.; Roy, V. A. L.; Sonar, P.; Wadgaonkar, P. P., Phenothiazine and carbazole substituted pyrene based electroluminescent organic semiconductors for OLED devices. *Journal of Materials Chemistry C* **2016,** *4* (5), 1009-1018.

47. Siraj, N.; Hasan, F.; Das, S.; Kiruri, L. W.; Steege Gall, K. E.; Baker, G. A.; Warner, I. M., Carbazole-Derived Group of Uniform Materials Based on Organic Salts: Solid State Fluorescent Analogues of Ionic Liquids for Potential Applications in Organic-Based Blue Light-Emitting Diodes. *J. of Phys. Chem. C* **2014,** *118* (5), 2312-2320.

48. Tao, Y.; Yang, C.; Qin, J., Organic host materials for phosphorescent organic light-emitting diodes. *Chemical Society Reviews* **2011,** *40* (5), 2943-2970.

49. Liu, J.; Liu, J.; Zhang, Z.; Xu, C.; Li, Q.; Zhou, K.; Dong, H.; Zhang, X.; Hu, W., Enhancing field-effect mobility and maintaining solid-state emission by incorporating 2,6-diphenyl substitution to 9,10-bis(phenylethynyl)anthracene. *Journal of Materials Chemistry C* **2017,** *5* (10), 2519-2523.

50. Kim, S.-K.; Yang, B.; Park, Y.-I.; Ma, Y.; Lee, J.-Y.; Kim, H.-J.; Park, J., Synthesis and electroluminescent properties of highly efficient anthracene derivatives with bulky side groups. *Organic Electronics* **2009,** *10* (5), 822-833.

51. Park, Y.-I.; Son, J.-H.; Kang, J.-S.; Kim, S.-K.; Lee, J.-H.; Park, J.-W., Synthesis and electroluminescence properties of novel deep blue emitting 6,12-dihydro-diindeno[1,2-b;1′,2′-e]pyrazine derivatives. *Chemical Communications* **2008,** (18), 2143-2145.

52. Tonzola, C. J.; Kulkarni, A. P.; Gifford, A. P.; Kaminsky, W.; Jenekhe, S. A., Blue-Light-Emitting Oligoquinolines: Synthesis, Properties, and High-Efficiency Blue-Light-Emitting Diodes. *Advanced Functional Materials* **2007,** *17* (6), 863-874.

53. Chen, W.-C.; Zhu, Z.-L.; Lee, C.-S., Organic Light-Emitting Diodes Based on Imidazole Semiconductors. *Advanced Optical Materials* **2018,** *6* (18), 1800258.

54. Paun, A.; Hadade, N.; Paraschivescu, C.; Matache, M., 1,3,4-Oxadiazoles as luminescent materials for organic light emitting diodes: Via cross-coupling reactions. *J. Mater. Chem. C* **2016,** *4*.

55. Li, C.; Fan, X.; Han, C.; Xu, H., A ternary phosphine oxide host featuring thermally activated delayed fluorescence for blue PHOLEDs with >20% EQE and extremely low roll-offs. *Journal of Materials Chemistry C* **2018,** *6* (25), 6747-6754.

56. De Silva, T. P. D.; Youm, S. G.; Tamas, G. G.; Yang, B.; Wang, C.-H.; Fronczek, F. R.; Sahasrabudhe, G.; Sterling, S.; Quarels, R. D.; Chhotaray, P. K.; Nesterov, E. E.; Warner, I. M., Pyrenylpyridines: Sky-Blue Emitters for Organic Light-Emitting Diodes. *ACS Omega* **2019,** *4* (16), 16867-16877.

57. Zhang, Q.; Xiang, S.; Huang, Z.; Sun, S.; Ye, S.; Lv, X.; Liu, W.; Guo, R.; Wang, L., Molecular engineering of pyrimidine-containing thermally activated delayed fluorescence emitters for highly efficient deep-blue (CIEy < 0.06) organic light-emitting diodes. *Dyes and Pigments* **2018,** *155*, 51-58.

58. Astruc, D.; Boisselier, E.; Ornelas, C., Dendrimers designed for functions: from physical, photophysical, and supramolecular properties to applications in sensing, catalysis, molecular electronics, photonics, and nanomedicine. *Chemical reviews* **2010,** *110* (4), 1857-1959.

59. Park, Y.-I.; Son, J.-H.; Kang, J.-S.; Kim, S.-K.; Lee, J.-H.; Park, J.-W., Synthesis and electroluminescence properties of novel deep blue emitting 6,12-dihydro-diindeno[1,2-b;1′,2′-e]pyrazine derivatives. *Chemical Communications* **2008,** (18), 2143-2145.

60. Birks, J., On the delayed fluorescence of pyrene solutions. *The Journal of Physical Chemistry* **1963,** *67* (10), 2199-2200.

61. Chercka, D.; Yoo, S.-J.; Baumgarten, M.; Kim, J.-J.; Müllen, K., Pyrene based materials for exceptionally deep blue OLEDs. *Journal of Materials Chemistry C* **2014,** *2* (43), 9083-9086.

62. Figueira-Duarte, T. M.; Mullen, K., Pyrene-based materials for organic electronics. *Chemical reviews* **2011,** *111* (11), 7260-7314.

63. Figueira-Duarte, T. M.; Müllen, K., Pyrene-Based Materials for Organic Electronics. *Chemical Reviews* **2011,** *111* (11), 7260-7314.

64. Birks, J. B.; Christophorou, L. G., Excimer fluorescence spectra of pyrene derivatives. *Spectrochimica Acta* **1963,** *19* (2), 401-410.

65. Yeh, C.-C.; Lee, M.-T.; Chen, H.-H.; Chen, C. H., 17.3: High-Performance Blue OLEDs Based on a Sterically Hindered Pyrene Host Material. *SID Symposium Digest of Technical Papers* **2004,** *35* (1), 788-791.

66. Trattnig, R.; Figueira-Duarte, T. M.; Lorbach, D.; Wiedemair, W.; Sax, S.; Winkler, S.; Vollmer, A.; Koch, N.; Manca, M.; Loi, M. A.; Baumgarten, M.; List, E. J. W.; Müllen,

K., Deep blue polymer light emitting diodes based on easy to synthesize, non-aggregating polypyrene. *Opt. Express* **2011,** *19* (S6), A1281-A1293.

67. Bernhardt, S.; Kastler, M.; Enkelmann, V.; Baumgarten, M.; Müllen, K., Pyrene as Chromophore and Electrophore: Encapsulation in a Rigid Polyphenylene Shell. *Chemistry – A European Journal* **2006,** *12* (23), 6117-6128.

68. Adams, E. M.; Wellen, B. A.; Thiraux, R.; Reddy, S. K.; Vidalis, A. S.; Paesani, F.; Allen, H. C., Sodium-carboxylate contact ion pair formation induces stabilization of palmitic acid monolayers at high pH. *Physical Chemistry Chemical Physics* **2017**.

69. Calvo-Castro, J.; McHugh, C. J., Exploring structure based charge transport relationships in phenyl diketopyrrolopyrrole single crystals using a 2D [small pi]-[small pi] dimer model system. *Journal of Materials Chemistry C* **2017**.

70. De Silva, T. P. D.; Youm, S. G.; Tamas, G. G.; Yang, B.; Wang, C.-H.; Fronczek, F. R.; Sahasrabudhe, G.; Sterling, S.; Quarels, R. D.; Chhotaray, P. K.; Nesterov, E. E.; Warner, I. M., Pyrenylpyridines: Sky-Blue Emitters for Organic Light-Emitting Diodes. *ACS Omega* **2019,** *4* (16), 16867-16877.

71. Schnaiter, M.; Horvath, H.; Möhler, O.; Naumann, K.-H.; Saathoff, H.; Schöck, O., UV-VIS-NIR spectral optical properties of soot and soot-containing aerosols. *Journal of Aerosol Science* **2003,** *34* (10), 1421-1444.

72. Turro, N. J.; Ramamurthy, V.; Scaiano, J. C., *Modern Molecular Photochemistry of Organic Molecules*. Viva Books, published by arrangement with University Science Books …: 2017.

73. Huang, Q., Basic principles of spectroscopy. **1971**.

74. Perkampus, H.-H., *UV-VIS Spectroscopy and its Applications*. Springer Science & Business Media: 2013.

75. Lakowicz, J. R., *Principles of fluorescence spectroscopy*. Springer Science & Business Media: 2013.

76. Murthy, K.; Virk, H. S. In *Luminescence phenomena: an introduction*, Defect and Diffusion Forum, Trans Tech Publ: 2014; pp 1-34.

77. Lakowicz, J. R., *Principles of fluorescence spectroscopy*. Springer Science & Business Media: 2013.

78. Albrecht, C., Joseph R. Lakowicz: Principles of fluorescence spectroscopy. *Analytical and Bioanalytical chemistry* **2008,** *390* (5), 1223-1224.

79. Wolfbeis, O. S., *Fluorescence spectroscopy: new methods and applications*. Springer Science & Business Media: 2012.

80. Permyakov, E. A., *Luminescent spectroscopy of proteins*. CRC press: 2018.

81. Andrews, D. L.; Demidov, A. A., *An introduction to laser spectroscopy*. Springer Science & Business Media: 2012.

82. Ozinskas, A. J., Principles of fluorescence immunoassay. In *Topics in fluorescence spectroscopy*, Springer: 2002; pp 449-496.

83. Chung, F. H., Quantitative interpretation of X-ray diffraction patterns of mixtures. II. Adiabatic principle of X-ray diffraction analysis of mixtures. *Journal of Applied Crystallography* **1974,** *7* (6), 526-531.

84. David, W. I.; Shankland, K.; Baerlocher, C.; McCusker, L., *Structure determination from powder diffraction data*. Oxford University Press on Demand: 2002; Vol. 13.

85. Černý, R.; Favre-Nicolin, V., Direct space methods of structure determination from powder diffraction: principles, guidelines and perspectives. *Zeitschrift für Kristallographie-Crystalline Materials* **2007,** *222* (3-4), 105-113.

86. Klug, H. P.; Alexander, L. E., X-ray diffraction procedures: for polycrystalline and amorphous materials. *X-Ray Diffraction Procedures: For Polycrystalline and Amorphous Materials, 2nd Edition, by Harold P. Klug, Leroy E. Alexander, pp. 992. ISBN 0-471-49369-4. Wiley-VCH, May 1974.* **1974**, 992.

87. Wang, P. In *Review and recent progress of handheld spectrometry at Thermo Fisher Scientific*, Next-Generation Spectroscopic Technologies VIII, International Society for Optics and Photonics: 2015; p 948204.

88. Chalmers, J. M.; Edwards, H. G.; Hargreaves, M. D., *Infrared and Raman spectroscopy in forensic science*. John Wiley & Sons: 2012.

89. Chalmers, J. M.; Edwards, H. G.; Hargreaves, M. D., *Infrared and Raman spectroscopy in forensic science*. John Wiley & Sons: 2012.

90. Siesler, H. W.; Ozaki, Y.; Kawata, S.; Heise, H. M., *Near-infrared spectroscopy: principles, instruments, applications*. John Wiley & Sons: 2008.

91. Rohman, A.; Man, Y. C., Fourier transform infrared (FTIR) spectroscopy for analysis of extra virgin olive oil adulterated with palm oil. *Food research international* **2010,** *43* (3), 886-892.

92. Faix, O., Fourier transform infrared spectroscopy. In *Methods in lignin chemistry*, Springer: 1992; pp 83-109.

93. Prime, R. B.; Bair, H. E.; Vyazovkin, S.; Gallagher, P. K.; Riga, A., Thermogravimetric analysis (TGA). *Thermal analysis of polymers: Fundamentals and applications* **2009**, 241-317.

94. Idris, S. S.; Rahman, N. A.; Ismail, K.; Alias, A. B.; Rashid, Z. A.; Aris, M. J., Investigation on thermochemical behaviour of low rank Malaysian coal, oil palm biomass and their blends during pyrolysis via thermogravimetric analysis (TGA). *Bioresource technology* **2010,** *101* (12), 4584-4592.

95. Ibraheem, N. A.; Hasan, M. M.; Khan, R. Z.; Mishra, P. K., Understanding color models: a review. *ARPN Journal of science and technology* **2012,** *2* (3), 265-275.

96. Koenderink, J. J., *Color for the Sciences*. The MIT Press: 2010.

97. Luo, M.; Hunt, R., The structure of the CIE 1997 colour appearance model (CIECAM97s). *Color Research & Application: Endorsed by Inter-Society Color Council, The Colour Group (Great Britain), Canadian Society for Color, Color Science Association of Japan,*

Dutch Society for the Study of Color, The Swedish Colour Centre Foundation, Colour Society of Australia, Centre Français de la Couleur **1998,** *23* (3), 138-146.

98. Zhu, S.; Meng, Q.; Wang, L.; Zhang, J.; Song, Y.; Jin, H.; Zhang, K.; Sun, H.; Wang, H.; Yang, B., Highly photoluminescent carbon dots for multicolor patterning, sensors, and bioimaging. *Angewandte Chemie* **2013,** *125* (14), 4045-4049.

99. Faklaris, O.; Garrot, D.; Joshi, V.; Druon, F.; Boudou, J. P.; Sauvage, T.; Georges, P.; Curmi, P. A.; Treussart, F., Detection of single photoluminescent diamond nanoparticles in cells and study of the internalization pathway. *Small* **2008,** *4* (12), 2236-2239.

100. Giridharagopal, R.; Rayermann, G.; Ginger, D., Electrical scanning probe microscopy on solar cell materials. *Scanning Probe Microscopy For Energy Research: Materials, Devices, And Applications* **2013,** *7*, 28.

101. Yip, H.-L.; Jen, A. K.-Y., Semi-transparent polymer solar cells for power generating window applications. In *Polymer Photovoltaics*, 2015; pp 352-375.

102. Shaheen, S. E.; Brabec, C. J.; Sariciftci, N. S.; Padinger, F.; Fromherz, T.; Hummelen, J. C., 2.5% efficient organic plastic solar cells. *Applied Physics Letters* **2001,** *78* (6), 841-843.

103. Chen, C.-Y.; Wang, M.; Li, J.-Y.; Pootrakulchote, N.; Alibabaei, L.; Ngoc-le, C.-h.; Decoppet, J.-D.; Tsai, J.-H.; Grätzel, C.; Wu, C.-G., Highly efficient light-harvesting ruthenium sensitizer for thin-film dye-sensitized solar cells. *ACS nano* **2009,** *3* (10), 3103-3109.

104. Kalyani, N. T.; Dhoble, S., Organic light emitting diodes: Energy saving lighting technology—A review. *Renewable and Sustainable Energy Reviews* **2012,** *16* (5), 2696-2723.

105. Shinar, J., *Organic light-emitting devices: a survey*. Springer Science & Business Media: 2013.

106. Kulkarni, A. P.; Tonzola, C. J.; Babel, A.; Jenekhe, S. A., Electron transport materials for organic light-emitting diodes. *Chemistry of materials* **2004,** *16* (23), 4556-4573.

107. Li, G.; Zhu, R.; Yang, Y., Polymer solar cells. *Nature photonics* **2012,** *6* (3), 153.

108. Sekine, C.; Tsubata, Y.; Yamada, T.; Kitano, M.; Doi, S., Recent progress of high performance polymer OLED and OPV materials for organic printed electronics. *Science and Technology of Advanced Materials* **2014,** *15* (3), 034203.

109. Youn, H.; Park, H. J.; Guo, L. J., Printed Nanostructures for Organic Photovoltaic Cells and Solution-Processed Polymer Light-Emitting Diodes. *Energy Technology* **2015,** *3* (4), 340-350.

110. Kim, J.-J.; Han, M.-K.; Noh, Y.-Y., Flexible OLEDs and organic electronics. *Semiconductor Science and Technology* **2011,** *26* (3), 030301.

111. Williams, J. G.; Develay, S.; Rochester, D. L.; Murphy, L., Optimising the luminescence of platinum (II) complexes and their application in organic light emitting devices (OLEDs). *Coordination Chemistry Reviews* **2008,** *252* (23-24), 2596-2611.

112. Baek, G.; Abe, K.; Kuo, A.; Kumomi, H.; Kanicki, J., Electrical properties and stability of dual-gate coplanar homojunction DC sputtered amorphous indium–gallium–zinc–oxide thin-film transistors and its application to AM-OLEDs. *IEEE Transactions on Electron Devices* **2011,** *58* (12), 4344-4353.

113. Zhao, Z.; Xu, X.; Wang, H.; Lu, P.; Yu, G.; Liu, Y., Zigzag molecules from pyrene-modified carbazole oligomers: synthesis, characterization, and application in OLEDs. *The Journal of organic chemistry* **2008,** *73* (2), 594-602.

114. Tampoia, M.; Abbracciavento, L.; Barberio, G.; Fabris, M.; Bizzaro, N., A new M23-based ELISA assay for anti-aquaporin 4 autoantibodies: diagnostic accuracy and clinical correlation. *Autoimmunity Highlights* **2019,** *10* (1), 5.

115. Mayoral, M. J.; Serrano-Molina, D.; Camacho-García, J.; Magdalena-Estirado, E.; Blanco-Lomas, M.; Fadaei, E.; González-Rodríguez, D., Understanding complex supramolecular landscapes: non-covalent macrocyclization equilibria examined by fluorescence resonance energy transfer. *Chemical Science* **2018,** *9* (40), 7809-7821.

116. Duffy, M. P.; Delaunay, W.; Bouit, P.-A.; Hissler, M., π-Conjugated phospholes and their incorporation into devices: components with a great deal of potential. *Chemical Society Reviews* **2016,** *45* (19), 5296-5310.

117. Moorthy, J. N.; Natarajan, P.; Venkatakrishnan, P.; Huang, D.-F.; Chow, T. J., Steric inhibition of π-stacking: 1, 3, 6, 8-tetraarylpyrenes as efficient blue emitters in organic light emitting diodes (OLEDs). *Organic letters* **2007,** *9* (25), 5215-5218.

118. Holder, E.; Langeveld, B. M.; Schubert, U. S., New trends in the use of transition metal–ligand complexes for applications in electroluminescent devices. *Advanced Materials* **2005,** *17* (9), 1109-1121.

119. Burrows, P.; Gu, G.; Bulovic, V.; Shen, Z.; Forrest, S.; Thompson, M., Achieving full-color organic light-emitting devices for lightweight, flat-panel displays. *IEEE Transactions on electron devices* **1997,** *44* (8), 1188-1203.

120. Friend, R.; Gymer, R.; Holmes, A.; Burroughes, J.; Marks, R.; Taliani, C.; Bradley, D.; Dos Santos, D.; Bredas, J.; Lögdlund, M., Electroluminescence in conjugated polymers. *nature* **1999,** *397* (6715), 121.

121. Lee, J.-H.; Chen, C.-H.; Lee, P.-H.; Lin, H.-Y.; Leung, M.-k.; Chiu, T.-L.; Lin, C.-F., Blue organic light-emitting diodes: current status, challenges, and future outlook. *Journal of Materials Chemistry C* **2019,** *7* (20), 5874-5888.

122. Reiherzer, J. C., White light emitting devices including both red and multi-phosphor blue-shifted-yellow solid state emitters. Google Patents: 2016.

123. Kulkarni, A. P.; Tonzola, C. J.; Babel, A.; Jenekhe, S. A., Electron Transport Materials for Organic Light-Emitting Diodes. *Chemistry of Materials* **2004,** *16* (23), 4556-4573.

124. Zhu, Y.; Kulkarni, A. P.; Jenekhe, S. A., Phenoxazine-Based Emissive Donor−Acceptor Materials for Efficient Organic Light-Emitting Diodes. *Chemistry of Materials* **2005,** *17* (21), 5225-5227.

125. Yao, J.; Ying, S.; Sun, Q.; Dai, Y.; Qiao, X.; Yang, D.; Chen, J.; Ma, D., High efficiency blue/green/yellow/red fluorescent organic light-emitting diodes sensitized by phosphors: general design rules and electroluminescence performance analysis. *Journal of Materials Chemistry C* **2019,** *7* (36), 11293-11302.

126. Salunke, J. K.; Sonar, P.; Wong, F. L.; Roy, V. A. L.; Lee, C. S.; Wadgaonkar, P. P., Pyrene based conjugated materials: synthesis, characterization and electroluminescent properties. *Physical Chemistry Chemical Physics* **2014,** *16* (42), 23320-23328.

127. Shih, P.-I.; Chiang, C.-L.; Dixit, A. K.; Chen, C.-K.; Yuan, M.-C.; Lee, R.-Y.; Chen, C.-T.; Diau, E. W.-G.; Shu, C.-F., Novel carbazole/fluorene hybrids: host materials for blue phosphorescent OLEDs. *Organic letters* **2006,** *8* (13), 2799-2802.

128. Siraj, N.; Warner, I. M.; De Silva, T. P. D., Carbazole-based gumbos for highly efficient blue OLEDs. US Patent App. 15/541,524: 2018.

129. Shi, J.; Tang, C. W., Anthracene derivatives for stable blue-emitting organic electroluminescence devices. *Applied physics letters* **2002,** *80* (17), 3201-3203.

130. Wen, S.-W.; Lee, M.-T.; Chen, C. H., Recent development of blue fluorescent OLED materials and devices. *Journal of display technology* **2005,** *1* (1), 90-99.

131. Kozma, E.; Mróz, W.; Villafiorita-Monteleone, F.; Galeotti, F.; Andicsová-Eckstein, A.; Catellani, M.; Botta, C., Perylene diimide derivatives as red and deep red-emitters for fully solution processable OLEDs. *RSC Advances* **2016,** *6* (66), 61175-61179.

132. Tang, C.; Liu, F.; Xia, Y.-J.; Lin, J.; Xie, L.-H.; Zhong, G.-Y.; Fan, Q.-L.; Huang, W., Fluorene-substituted pyrenes—Novel pyrene derivatives as emitters in nondoped blue OLEDs. *Organic electronics* **2006,** *7* (3), 155-162.

133. Lo, M. Y.; Zhen, C.; Lauters, M.; Jabbour, G. E.; Sellinger, A., Organic− inorganic hybrids based on pyrene functionalized octavinylsilsesquioxane cores for application in OLEDs. *Journal of the American Chemical Society* **2007,** *129* (18), 5808-5809.

134. Chercka, D.; Yoo, S.-J.; Baumgarten, M.; Kim, J.-J.; Müllen, K., Pyrene based materials for exceptionally deep blue OLEDs. *Journal of Materials Chemistry C* **2014,** *2* (43), 9083-9086.

135. Salunke, J. K.; Sonar, P.; Wong, F. L.; Roy, V. A. L.; Lee, C. S.; Wadgaonkar, P. P., Pyrene based conjugated materials: synthesis, characterization and electroluminescent properties. *Physical Chemistry Chemical Physics* **2014,** *16* (42), 23320-23328.

136. Yao, J.; Ying, S.; Sun, Q.; Dai, Y.; Qiao, X.; Yang, D.; Chen, J.; Ma, D., High efficiency blue/green/yellow/red fluorescent organic light-emitting diodes sensitized by phosphors: general design rules and electroluminescence performance analysis. *Journal of Materials Chemistry C* **2019,** *7* (36), 11293-11302.

137. Kotchapradist, P.; Prachumrak, N.; Tarsang, R.; Jungsuttiwong, S.; Keawin, T.; Sudyoadsuk, T.; Promarak, V., Pyrene-functionalized carbazole derivatives as non-doped blue emitters for highly efficient blue organic light-emitting diodes. *Journal of Materials Chemistry C* **2013,** *1* (32), 4916-4924.

138. Zhan, Y.; Peng, J.; Ye, K.; Xue, P.; Lu, R., Pyrene functionalized triphenylamine-based dyes: synthesis, photophysical properties and applications in OLEDs. *Organic & Biomolecular Chemistry* **2013,** *11* (39), 6814-6823.

139. De Silva, T. P. D.; Youm, S. G.; Tamas, G. G.; Yang, B.; Wang, C.-H.; Fronczek, F. R.; Sahasrabudhe, G.; Sterling, S.; Quarels, R. D.; Chhotaray, P. K.; Nesterov, E. E.; Warner, I. M., Pyrenylpyridines: Sky-Blue Emitters for Organic Light-Emitting Diodes. *ACS Omega* **2019,** *4* (16), 16867-16877.

140. Figueira-Duarte, T. M.; Mullen, K., Pyrene-based materials for organic electronics. *Chemical reviews* **2011,** *111* (11), 7260-7314.

141. Hong, Y.; Lam, J. W.; Tang, B. Z., Aggregation-induced emission. *Chemical Society Reviews* **2011,** *40* (11), 5361-5388.

142. Salunke, J. K.; Sonar, P.; Wong, F. L.; Roy, V. A. L.; Lee, C. S.; Wadgaonkar, P. P., Pyrene based conjugated materials: synthesis, characterization and electroluminescent properties. *Physical Chemistry Chemical Physics* **2014,** *16* (42), 23320-23328.

143. Banal, J. L.; White, J. M.; Lam, T. W.; Blakers, A. W.; Ghiggino, K. P.; Wong, W. W., A Transparent Planar Concentrator Using Aggregates of gem-Pyrene Ethenes. *Advanced Energy Materials* **2015,** *5* (19), 1500818.

144. De Silva, T. P. D.; Youm, S. G.; Tamas, G. G.; Yang, B.; Wang, C.-H.; Fronczek, F. R.; Sahasrabudhe, G.; Sterling, S.; Quarels, R. D.; Chhotaray, P. K.; Nesterov, E. E.; Warner, I. M., Pyrenylpyridines: Sky-Blue Emitters for Organic Light-Emitting Diodes. *ACS Omega* **2019,** *4* (16), 16867-16877.

145. Johnson, E. R.; Keinan, S.; Mori-Sánchez, P.; Contreras-García, J.; Cohen, A. J.; Yang, W., Revealing Noncovalent Interactions. *Journal of the American Chemical Society* **2010,** *132* (18), 6498-6506.

146. De Silva, T. P. D.; Youm, S. G.; Tamas, G. G.; Yang, B.; Wang, C.-H.; Fronczek, F. R.; Sahasrabudhe, G.; Sterling, S.; Quarels, R. D.; Chhotaray, P. K.; Nesterov, E. E.; Warner, I. M., Pyrenylpyridines: Sky-Blue Emitters for Organic Light-Emitting Diodes. *ACS Omega* **2019,** *4* (16), 16867-16877.

147. Liu, Y.; Bai, Q.; Li, J.; Zhang, S.; Zhang, C.; Lu, F.; Yang, B.; Lu, P., Efficient pyrene-imidazole derivatives for organic light-emitting diodes. *RSC Advances* **2016,** *6* (21), 17239-17245.

148. Chidirala, S.; Ulla, H.; Valaboju, A.; Kiran, M. R.; Mohanty, M. E.; Satyanarayan, M. N.; Umesh, G.; Bhanuprakash, K.; Rao, V. J., Pyrene–Oxadiazoles for Organic Light-Emitting Diodes: Triplet to Singlet Energy Transfer and Role of Hole-Injection/Hole-Blocking Materials. *The Journal of Organic Chemistry* **2016,** *81* (2), 603-614.

149. Cho, S.-J.; Lee, C.-M., Condensed cyclic compound and organic light-emitting device including the same. Google Patents: 2015.

150. Klimm, D., Electronic materials with a wide band gap: recent developments. *IUCrJ* **2014,** *1* (Pt 5), 281-290.

151. Chidirala, S.; Ulla, H.; Valaboju, A.; Kiran, M. R.; Mohanty, M. E.; Satyanarayan, M.; Umesh, G.; Bhanuprakash, K.; Rao, V. J., Pyrene–oxadiazoles for organic light-emitting diodes: triplet to singlet energy transfer and role of hole-injection/hole-blocking materials. *The Journal of organic chemistry* **2015,** *81* (2), 603-614.

152. Kwak, K.; Cho, K.; Kim, S., Analysis of thermal degradation of organic light-emitting diodes with infrared imaging and impedance spectroscopy. *Opt. Express* **2013,** *21* (24), 29558-29566.

153. Qiao, J.; Zhao, J.; Liu, Q.; Xia, Z., Recent advances in solid-state LED phosphors with thermally stable luminescence. *Journal of Rare Earths* **2019,** *37* (6), 565-572.

154. Mori, T.; Mitsuoka, T.; Ishii, M.; Fujikawa, H.; Taga, Y., Improving the thermal stability of organic light-emitting diodes by using a modified phthalocyanine layer. *Applied physics letters* **2002,** *80* (21), 3895-3897.

155. Evans, O. R.; Lin, W., Crystal engineering of NLO materials based on metal− organic coordination networks. *Accounts of Chemical Research* **2002,** *35* (7), 511-522.

156. De Silva, T. P. D.; Youm, S. G.; Tamas, G. G.; Yang, B.; Wang, C.-H.; Fronczek, F. R.; Sahasrabudhe, G.; Sterling, S.; Quarels, R. D.; Chhotaray, P. K.; Nesterov, E. E.; Warner, I. M. Pyrenylpyridines: Sky-Blue Emitters for Organic Light-Emitting Diodes *ACS omega* [Online], 2019, p. 16867-16877.

157. Zhang, Y.; Lai, S.-L.; Tong, Q.-X.; Lo, M.-F.; Ng, T.-W.; Chan, M.-Y.; Wen, Z.-C.; He, J.; Jeff, K.-S.; Tang, X.-L., High efficiency nondoped deep-blue organic light emitting devices based on imidazole-π-triphenylamine derivatives. *Chemistry of Materials* **2011,** *24* (1), 61-70.

158. Chen, J.; Tang, W.; Xin, L.; Shi, Q., Band gap characterization and photoluminescence properties of SiC nanowires. *Applied Physics A* **2011,** *102* (1), 213-217.

159. Manandhar, E.; Wallace, K. J., Host–guest chemistry of pyrene-based molecular receptors. *Inorganica Chimica Acta* **2012,** *381*, 15-43.

160. Song, H.-Z.; Bao, X.-M.; Li, N.-S.; Zhang, J.-Y., Relation between electroluminescence and photoluminescence of Si+-implanted SiO2. *Journal of Applied Physics* **1997,** *82* (8), 4028-4032.

161. Andersson, M. R.; Yu, G.; Heeger, A. J., Photoluminescence and electroluminescence of films from soluble PPV-polymers. *Synthetic Metals* **1997,** *85* (1), 1275-1276.

162. Hong, K.; Lee, J.-L., Recent developments in light extraction technologies of organic light emitting diodes. *Electronic Materials Letters* **2011,** *7* (2), 77-91.

163. Komatsu, R.; Sasabe, H.; Kido, J., Recent progress of pyrimidine derivatives for high-performance organic light-emitting devices. *Journal of Photonics for Energy* **2018,** *8* (3), 032108.

164. Golec, B.; Nawara, K.; Gorski, A.; Thummel, R. P.; Herbich, J.; Waluk, J., Combined effect of hydrogen bonding interactions and freezing of rotameric equilibrium on the enhancement of photostability. *Physical Chemistry Chemical Physics* **2018,** *20* (19), 13306-13315.

VITA

John Mathaga was born and raised in Kenya. He attended Mary Mother of Grace high school in Laikipia county, where he was inspired to pursue his interest in chemistry by his chemistry teacher Mr. Muchemi. John began his undergraduate studies in Kenyatta University which is in Nairobi county, Kenya in 2000. I spring 2014, John started his graduate studies in chemistry at Louisiana State University where he was mentored by Professor Isiah Warner. John intend to graduate with the degree of Masters of Science in chemistry from Louisiana State University in summer 2020.

Publications

Taping, L.; Yaowen, C.; Mathaga, J.; Kumar, R.; Kuroda, D. G. "Hydration and Vibrational Dynamics of Betaine (N, N, N-trimethylglycine)." J. Chem. Phys. **2015,** 142, 212438

Mathaga, J. K.; Thoruwa, T. F. N.; Muthakia, G. K. "Activation of Spent Bleaching Earth for Dehumidification Application." J. Wajbas., **2013**, 1, 1-8.

Presentations

Mathaga, J.; "Ultrasensitive Ebola Virus Detection Based on Electroluminescent Nanospheres and Immunomagnetic Separation." April 2018 Analytical Seminal. Louisiana State University, Baton Rouge, LA.

Mathaga, J.; Rocío P.; Sudhir R.; Isiah M. W. "Novel pyrimidine-pyrene semiconductors for blue organic light-emitting device." March 2018, 255th America Chemical Society (ACS) meeting. Convention Center, New Orleans, LA

Mathaga, J.; Tanping, L.; Yaowen, C.; Kumar, R.; Kuroda, D. G. "Hydration and Vibrational Dynamics of Betaine (N, N, N-trimethylglycine)." April 2015, LA-SIGMA Technical Conference. Marriott, Baton Rouge, LA

Mathaga, J.; Tanping, L.; Yaowen, C.; Kumar, R.; Kuroda, D. G. "Hydration and Vibrational Dynamics of Betaine (N, N, N-trimethylglycine)." March 2015, 89th Annual Meeting of the Louisiana Academy of Sciences. Nicholls State University, LA.

Mathaga, J. K. "Calcium Chloride Supported on Regenerated Spent Bleaching Earth (RSBE) as Potential Adsorptive Material for Air Dehumidification Application" September 2011, Graduate Thesis Defense, Kenyatta University, Nairobi, Kenya